that reported previously (22). In the present study, we used frozen sections, which were usually taken from an area away from the center of the main tumor because the main lesions were fixed with formalin for accurate diagnosis and clinical decision making. Therefore, formalin-fixed, paraffin-embedded, and frozen sections may show significant differences due to the locations within the tumor from which they are most likely taken. In addition, in studies of formalin-fixed and paraffin-embedded samples, most dysplastic lesions are typically selected from many sections, whereas the sections from frozen samples are very limited. Therefore, the studies with formalin-fixed and paraffin-embedded samples typically contain a greater proportion of higher-grade IPMNs than studies with frozen samples. This may underlie the differences in proportion of IPMN type because pancreaticobiliary or intestinal phenotypes are often correlated with high-grade atypia. In the present study, pancreaticobiliary-type and oncocytic-type IPMNs were not included because such samples were unavailable, possibly due to the rarity of such IPMN types in Japan or because we selected nonmalignant IPMN. Representative photomicrographs of gastric-type and intestinal-type IPMNs are shown in Fig. 1.

Statistical Analyses. Data were analyzed by Kruskal-Wallis test if comparisons involved three groups and by Mann-Whitney *U* test and Spearman rank correlation test if comparisons involved two groups because normal distributions were not obtained. Statistical significance was defined as $P < 0.05$. Because we did multiple comparisons, we used Bonferroni correction; therefore, the adjusted significance levels were $P < 0.008$ for microdissection data and $P < 0.017$ for pancreatic juice data. The patient distribution was examined by χ^2 test for categorical variables and by Kruskal-Wallis test for continuous variables. The optimal cutoff points for each marker for discriminating between pancreatic carcinoma or IPMN and chronic pancreatitis were sought by constructing receiver operating characteristic (ROC) curves, which were generated by calculating the sensitivities and specificities of data for each marker at several predetermined cutoff points with the MedCalc statistical software package, version 7.6 (MedCalc, Mariakerke, Belgium; ref. 23).

Results

Quantitative Analysis of S100A6 Expression in IDC Cells, Nonmalignant IPMN Cells, PAE Cells, and Normal Epithelial Cells. In our previous study, we evaluated *S100A6* expression in normal pancreas bulk tissues and microdissected PanIN and normal ductal epithelial cells as counterparts of pancreatic cancer bulk tissues and microdissected IDC cells, respectively (5). Then, we found that pancreatic cancer bulk tissues expressed significantly higher levels of *S100A6* than did normal pancreas bulk tissues and also found that microdissected IDC, PanIN, and normal ductal cells expressed significantly different levels of *S100A6* (5).

In the clinical setting, however, it is important to distinguish pancreatic cancer from benign diseases, such as chronic pancreatitis and nonmalignant IPMN. IPMN and chronic pancreatitis samples frequently show changes in expression of tumor-related genes similar to those in pancreatic cancers (24-27). Thus, to determine whether *S100A6* is differentially expressed between pancreatic cancer, nonmalignant IPMN, and chronic pancreatitis, we did laser microdissection to isolate IDC cells, nonmalignant IPMN cells, PAE cells, and normal epithelial cells and quantified *S100A6* expression in each cell type with one-step quantitative real-time RT-PCR with gene-specific priming. As shown in Fig. 2, IDC cells and IPMN cells expressed significantly higher levels of *S100A6* than did PAE cells and normal epithelial cells (IDC or IPMN versus PAE cells or normal epithelial cells; $P < 0.0001$). IDC cells expressed higher levels of *S100A6* than did nonmalignant IPMN cells; however, this difference was not statistically significant. PAE cells expressed higher levels of *S100A6* than did normal epithelial cells, but this difference also was not statistically significant.

Nonmalignant IPMN is considered to be a precursor lesion of a subset of pancreatic cancer. It was reported that a subset of PAE cells has the potential to progress to pancreatic cancer, although this is very rare (10, 11). PanIN is also a common precursor lesion of pancreatic cancer (9). We reported previously that PanIN cells expressed higher levels of *S100A6* than did normal epithelial cells and lower levels than did IDC cells (5), which was consistent with the results of an immunohistochemical study reported by Vimalachandran et al. (6). Taken together, these data suggest that alteration of *S100A6* expression occurs at a very early stage of pancreatic carcinogenesis and that expression of *S100A6* increases in a stepwise manner during carcinogenesis.

Quantitative Analysis of *S100A6* mRNA Expression in Pancreatic Juice. The results of our microdissection-based analyses of isolated cells suggest that *S100A6* is a promising diagnostic marker to distinguish pancreatic cancer from chronic pancreatitis and nonmalignant IPMN. We analyzed *S100A6* mRNA levels in 93 pancreatic juice samples from patients with various pancreatic diseases. The baseline characteristics of the patients included in the present study are shown in Table 2. The distribution of patients did not

Gastric type Intestinal type

Figure 1. Representative photomicrographs of gastric-type and intestinal-type IPMN. H&E stain. *Inset*, lower magnification.

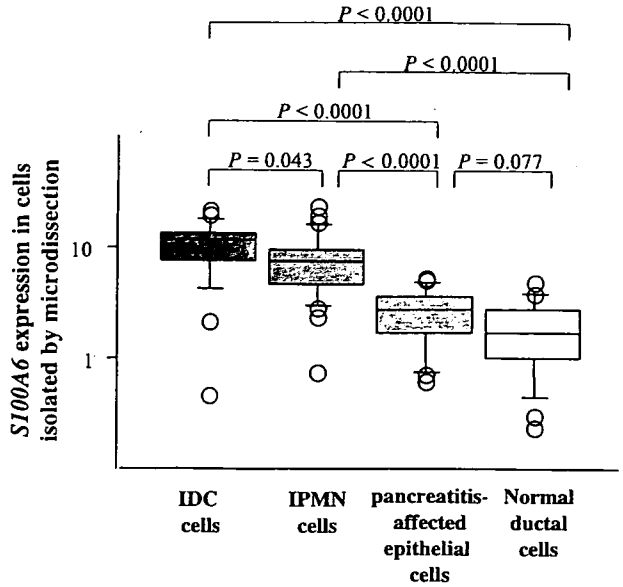

Figure 2. Microdissection-based quantitative analysis of *S100A6*. We isolated IDC cells, nonmalignant IPMN cells, PAE cells, and normal epithelial cells from frozen sections by microdissection and did one-step quantitative real-time RT-PCR with gene-specific priming to analyze expression of *S100A6* in these cells. Expression of S100A6 was normalized to that of *β-actin*. We found that IDC cells and IPMN cells express significantly higher levels of *S100A6* than do PAE cells and normal ductal epithelial cells. The median value of *S100A6* in IDC cells was higher than that in IPMN cells, although the difference was not statistically significant ($P = 0.043$). The median value of *S100A6* in PAE cells was higher than that in normal epithelial cells; however, the difference was not statistically significant ($P = 0.077$).

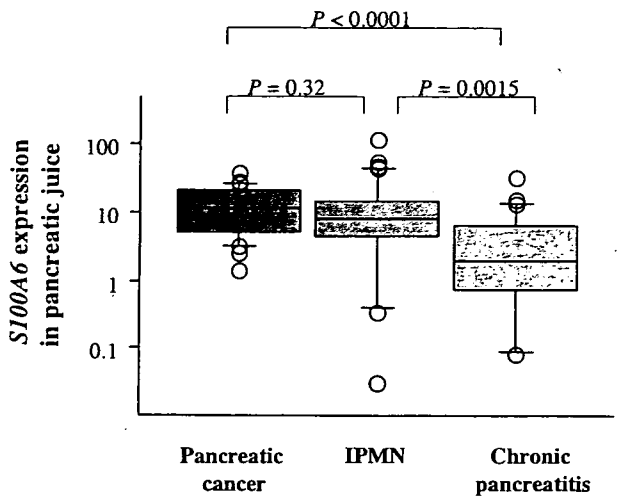

Figure 3. Quantification of *S100A6* mRNA expression in pancreatic juice. Expression of *S100A6* in pancreatic juice samples was analyzed by one-step quantitative real-time RT-PCR with gene-specific priming and short amplicons and normalized to that of *β-actin*. *S100A6* expression differed significantly between pancreatic juice from patients with cancer and those with chronic pancreatitis ($P < 0.0001$) and between pancreatic juice samples from patients with IPMN and those with chronic pancreatitis ($P = 0.0015$) after Bonferroni correction (*, $P < 0.017$). However, S100A6 expression did not differ significantly between pancreatic juice samples from patients with cancer and those with IPMN ($P = 0.32$).

differ significantly for age, sex, or comorbid conditions between patients with pancreatic cancer, nonmalignant IPMN, and chronic pancreatitis. Expression of *S100A6* was significantly higher in pancreatic cancer and IPMN samples than in chronic pancreatitis samples after Bonferroni correction ($P < 0.0001$ for pancreatic cancer versus chronic pancreatitis; $P = 0.0015$ for IPMN versus chronic pancreatitis; Fig. 3). However, *S100A6* expression did not differ significantly between pancreatic cancer and IPMN samples ($P = 0.32$; Fig. 3). To investigate *S100A6* mRNA levels in pancreatic juice from normal pancreata, we analyzed five pancreatic juice samples from patients with pancreata, which were confirmed to be normal by endoscopic retrograde cholangiopancreatography, endoscopic ultrasound, and/or computer tomography. We found that *S100A6* mRNA levels were undetectable or extremely low in pancreatic juice samples from normal pancreata compared with levels in neoplastic samples. *S100A6* mRNA levels in normal pancreatic juice were similar to those of pancreatic juice samples from pancreatitis-affected pancreata (data not shown).

Table 2. Baseline characteristics of the study population

	Pancreatic cancer	Nonmalignant IPMN*	Chronic pancreatitis	P†
Age (25%-median-75%), y	57-66-73	55-68-71	54-64.5-75	0.6
Sex (M/F ratio)	1.36	1.06	3.00	0.4
Comorbid conditions (%)				
Cardiovascular disease	19.2	22.9	17.8	0.88
Diabetes	23.1	28.5	21.4	0.79
Pulmonary disease	15.4	11.4	10.7	0.8
Cytology‡ (%)				
I-II	53.8	90.9	100	<0.0001
III	34.6	9.1	0	
IV-V	11.5	0	0	
Stage§ of pancreatic cancer (%)				
I-III	19.2			
IVa and IVb	80.7			
Etiology of pancreatitis (%)				
Alcoholic			42.9	
Idiopathic			32.1	
Other			25	
Relative expression of S100A6 (25%-median-75%)	5.2-11.3-21.0	4.2-8.2-14.8	0.7-1.7-4.1	<0.0001

*Intraductal papillary mucinous neoplasm.
†For continuous variables: P for Kruskal-Wallis test. For categorical variables: P for χ^2 test.
‡Cytologic classification was as described in previously (18).
§Pancreatic cancer was staged according to Japan Pancreas Society Classification (17).

As shown in Table 2, our pancreatic juice analyses included 5 (19.2%) samples from patients with stage I, II, or III pancreatic cancers and 21 (80.7%) samples from patients with stage IVa and IVb pancreatic cancers. This study also included pancreatic juice samples from patients with chronic pancreatitis with different etiologies (Table 2). However, there were no significant differences in *S100A6* expression between different stages of pancreatic cancers ($P = 0.45$) or between different etiologies of chronic pancreatitis ($P = 0.36$). In the present study, cytologic class IV or V was considered positive for a diagnosis of malignancy. The cytologic sensitivity for diagnosis of pancreatic cancer was only 11.5%, although the specificity was 100% (Table 2). The distribution of atypical grades, including class I or II, class III, and class IV or V, was significantly different between patients with pancreatic cancer, nonmalignant IPMN, and chronic pancreatitis ($P < 0.0001$; Table 2). The distribution of atypical grades was significantly different between patients with pancreatic cancer and those with chronic pancreatitis ($P = 0.0003$) and between patients with pancreatic cancer and those with nonmalignant IPMN ($P = 0.004$). However, there was no significant difference in the distribution of atypical grades between patients with nonmalignant IPMN and chronic pancreatitis ($P = 0.11$). We also examined the correlation between *S100A6* expression and cytologic evaluation and found no significant correlation ($P = 0.31$).

ROC curves for *S100A6* expressions are shown in Fig. 4. The sensitivity of the S100A6 was determined at several specificity levels. The area under the ROC curve was 0.864 for pancreatic cancer versus chronic pancreatitis [95% confidence interval (95% CI), 0.746-0.941] and 0.749 for IPMN versus chronic pancreatitis (95% CI, 0.615-0.855). The area under the ROC curve was 0.555 for pancreatic cancer versus IPMN (95% CI, 0.416-0.688). In particular, a significant difference between the areas for pancreatic cancer versus chronic pancreatitis and pancreatic cancer versus IPMN was observed (difference between areas, 0.309; 95% CI, 0.178-0.440; $P < 0.001$). These data indicate that measurements of *S100A6* mRNA levels in pancreatic juice may provide some advantage in discriminating pancreatic cancer or IPMN from chronic pancreatitis but not in discriminating pancreatic cancer from IPMN.

Discussion

In the present study, microdissection-based analyses revealed that IDC, nonmalignant IPMN, PAE, and normal epithelial cells expressed different levels of *S100A6*. Previously, we reported that IDC, PanIN, and normal epithelial cells expressed different levels of *S100A6* (5). These data suggest that expression of *S100A6* is increased in a stepwise manner during pancreatic carcinogenesis. The present pancreatic juice analyses revealed that the levels of *S100A6* in pancreatic cancer and IPMN juice samples were significantly higher than those in chronic pancreatitis-juice samples. However, the levels of *S100A6* in pancreatic juice did not differ between pancreatic cancer and IPMN juice samples, which was inconsistent with the results of the present microdissection-based analyses. Apparently, contamination of pancreatic cancer juice samples with premalignant cells could reduce *S100A6* levels measured in total cell pellets from pancreatic juice samples. Thus, to examine the true levels of *S100A6* in highly dysplastic cells in pancreatic juice samples, microdissection of cell pellets from pancreatic juice samples is needed. Such studies are presently under way in our laboratory.

Several pancreatic juice markers, including *k-ras* mutations, telomerase activity, and *hTERT* mRNA, have been reported (16, 28, 29). Recently, mutations of *k-ras* in pancreatitis-affected pancreata and pancreatic cancer were reported (30). Because *k-ras* mutation analysis is qualitative, it may be difficult to monitor the progression of carcinogenesis, whereas the present *S100A6* mRNA analysis is quantitative. We reported previously that quantitative analysis of telomerase activity is useful for differentiation of pancreatic cancer from nonmalignant IPMN or chronic pancreatitis (16, 29). However, there is no way to check sample quality for telomerase activity assays; therefore, it is difficult to use this assay in routine clinical settings. We also reported that quantitative analysis of *hTERT* mRNA, which is a subunit of telomerase, is useful for distinguishing pancreatic cancer from nonmalignant IPMN (31). Although we can easily check the quality of RNAs, our results suggested that *hTERT* analysis is not useful for distinguishing pancreatic cancer from chronic pancreatitis because relatively high levels of *hTERT* mRNA are expressed by activated lymphocytes in chronic pancreatitis-related pancreatic juice. In the present study, we found that pancreatic cancer and nonmalignant IPMN expressed significantly higher levels of *S100A6* than did chronic pancreatitis-related pancreatic juice samples. Apparently, activation of telomerase or overexpression of *hTERT* mRNA occurs at a later stage of pancreatic carcinogenesis, whereas overexpression of *S100A6* may occur at an early stage of pancreatic carcinogenesis and may increase in a stepwise manner during the progression of pancreatic carcinogenesis. Therefore, compared with telomerase activity and *hTERT* mRNA assays, quantitative analysis of *S100A6* is especially useful for monitoring the progression of carcinogenesis in individuals with high risk of pancreatic cancer, such as those with a familial history or chronic pancreatitis, or for screening individuals with high-risk lesions that may progress to pancreatic cancer.

To date, no single biomarker has been proven to have sufficient diagnostic accuracy to serve as a stand-alone means for early detection and diagnosis of cancer. Thus, biomarkers can be of significant clinical value by providing evidence to

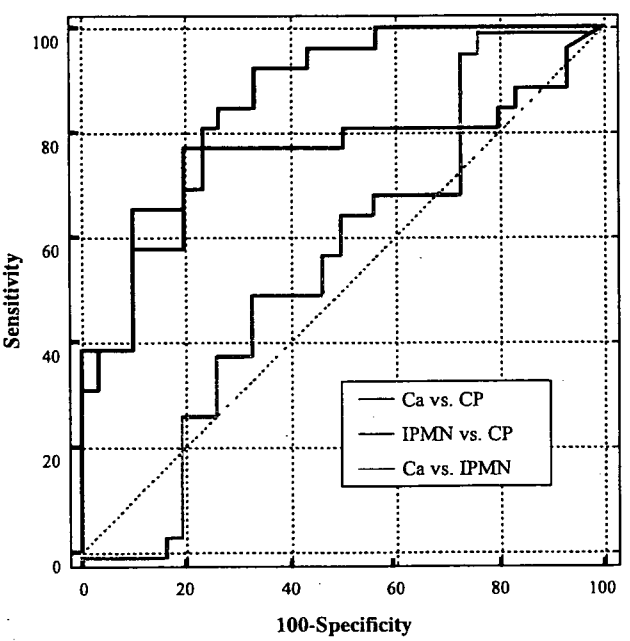

Figure 4. ROC curve analyses of S100A6 expression in pancreatic juice samples. Sensitivity of *S100A6* analysis was determined at several specificity levels. The areas under the ROC curve were 0.864 for pancreatic cancer versus chronic pancreatitis (95% CI, 0.746-0.941) and 0.749 for IPMN versus chronic pancreatitis (95% CI, 0.615-0.855). The area under the ROC curve was 0.555 for pancreatic cancer versus IPMN (95% CI, 0.416-0.688). The results of ROC curve analyses suggest that *S100A6* expression status can be used to differentiate pancreatic cancer or IPMN from chronic pancreatitis. *Ca*, pancreatic cancer; *CP*, chronic pancreatitis.

suspect cancer or, when combined with other clinical data, to aid in differential diagnosis. In the present study, the *S100A6* analyses of pancreatic juice yielded statistically significant differences between neoplastic samples, such as pancreatic cancer and nonmalignant IPMN and chronic pancreatitis samples, and our microdissection analyses revealed that expression of *S100A6* is increased in a stepwise manner during pancreatic carcinogenesis. Therefore, *S100A6* analysis of pancreatic juice may aid in differential diagnosis if combined with other clinical data and may have some advantages to detect or screen for pancreatic cancer and to follow up with individuals with high-risk factors, such as familial pancreatic cancer.

Acknowledgments

We thank M. Ohta (Department of Clinical Pathology, Kyushu University) for skillful cytologic examination and analysis.

References

1. Jemal A, Murray T, Samuels A, Ghafoor A, Ward E, Thun MJ. Cancer statistics, 2003. CA Cancer J Clin 2003;53:5–26.
2. Taylor B. Carcinoma of the head of the pancreas versus chronic pancreatitis: diagnostic dilemma with significant consequences. World J Surg 2003;27: 1249–57.
3. Ohhashi K, Murakami F, Maruyama M, et al. Four cases of mucous secreting pancreatic cancer [in Japanese with English abstract]. Prog Dig Endosc 1982; 203:348–351.
4. Yamaguchi K, Ohuchida J, Ohtsuka T, Nakano K, Tanaka M. Intraductal papillary-mucinous tumor of the pancreas concomitant with ductal carcinoma of the pancreas. Pancreatology 2002;2:484–90.
5. Ohuchida K, Mizumoto K, Ishikawa N, et al. The role of S100A6 in pancreatic cancer development and its clinical implication as a diagnostic marker and therapeutic target. Clin Cancer Res 2005;11:7785–93.
6. Vimalachandran D, Greenhalf W, Thompson C, et al. High nuclear S100A6 (calcyclin) is significantly associated with poor survival in pancreatic cancer patients. Cancer Res 2005;65:3218–25.
7. Logsdon CD, Simeone DM, Binkley C, et al. Molecular profiling of pancreatic adenocarcinoma and chronic pancreatitis identifies multiple genes differentially regulated in pancreatic cancer. Cancer Res 2003;63: 2649–57.
8. Breen EC, Tang K. Calcyclin (S100A6) regulates pulmonary fibroblast proliferation, morphology, and cytoskeletal organization *in vitro*. J Cell Biochem 2003;88:848–54.
9. Hruban RH, Adsay NV, Albores-Saavedra J, et al. Pancreatic intraepithelial neoplasia: a new nomenclature and classification system for pancreatic duct lesions. Am J Surg Pathol 2001;25:579–86.
10. Lowenfels AB, Maisonneuve P, Cavallini G, et al. Pancreatitis and the risk of pancreatic cancer. International Pancreatitis Study Group. N Engl J Med 1993;328:1433–7.
11. Karlson BM, Ekbom A, Josefsson S, McLaughlin JK, Fraumeni JF, Jr., Nyren O. The risk of pancreatic cancer following pancreatitis: an association due to confounding? Gastroenterology 1997;113:587–92.
12. Antonov J, Goldstein DR, Oberli A, et al. Reliable gene expression measurements from degraded RNA by quantitative real-time PCR depend on short amplicons and a proper normalization. Lab Invest 2005;85:1040–50.
13. Lekanne Deprez RH, Fijnvandraat AC, Ruijter JM, Moorman AF. Sensitivity and accuracy of quantitative real-time polymerase chain reaction using SYBR Green I depends on cDNA synthesis conditions. Anal Biochem 2002; 307:63–9.
14. Lewis F, Maughan NJ, Smith V, Hillan K, Quirke P. Unlocking the archive—gene expression in paraffin-embedded tissue. J Pathol 2001;195:66–71.
15. Ohuchida K, Mizumoto K, Yamada D, et al. Quantitative analysis of MUC1 and MUC5AC mRNA in pancreatic juice for preoperative diagnosis of pancreatic cancer. Int J Cancer 2006;118:405–11.
16. Ohuchida K, Mizumoto K, Ogura Y, et al. Quantitative assessment of telomerase activity and human telomerase reverse transcriptase messenger RNA levels in pancreatic juice samples for the diagnosis of pancreatic cancer. Clin Cancer Res 2005;11:2285–92.
17. Japan Pancreas Society. Classification of pancreatic carcinoma. Second English Edition. Tokyo: Kanehara & Co., Ltd.; 2003.
18. Yamaguchi K, Nakamura M, Shirahane K, et al. Pancreatic juice cytology in IPMN of the pancreas. Pancreatology 2005;5:416–21; discussion 21.
19. Tachikawa T, Irie T. A new molecular biology approach in morphology: basic method and application of laser microdissection. Med Electron Microsc 2004;37:82–8.
20. World Health Organization classification of tumors: pathology and genetics of tumors of the digestive system. Lyon: IARC Press; 2000.
21. Furukawa T, Kloppel G, Volkan Adsay N, et al. Classification of types of intraductal papillary-mucinous neoplasm of the pancreas: a consensus study. Virchows Arch 2005;447:794–9.
22. Adsay NV, Merati K, Basturk O, et al. Pathologically and biologically distinct types of epithelium in intraductal papillary mucinous neoplasms: delineation of an "intestinal" pathway of carcinogenesis in the pancreas. Am J Surg Pathol 2004;28:839–48.
23. Zweig MH, Campbell G. Receiver-operating characteristic (ROC) plots: a fundamental evaluation tool in clinical medicine. Clin Chem 1993;39: 561–77.
24. Biankin AV, Biankin SA, Kench JG, et al. Aberrant p16(INK4A) and DPC4/Smad4 expression in intraductal papillary mucinous tumours of the pancreas is associated with invasive ductal adenocarcinoma. Gut 2002;50: 861–8.
25. Soldini D, Gugger M, Burckhardt E, Kappeler A, Laissue JA, Mazzucchelli L. Progressive genomic alterations in intraductal papillary mucinous tumours of the pancreas and morphologically similar lesions of the pancreatic ducts. J Pathol 2003;199:453–61.
26. Hermanova M, Nenutil R, Kren L, Feit J, Pavlovsky Z, Dite P. Proliferative activity in pancreatic intraepithelial neoplasias of chronic pancreatitis resection specimens: detection of a high-risk lesion. Neoplasma 2004;51: 400–4.
27. Rosty C, Geradts J, Sato N, et al. p16 Inactivation in pancreatic intraepithelial neoplasias (PanINs) arising in patients with chronic pancreatitis. Am J Surg Pathol 2003;27:1495–501.
28. Tada M, Omata M, Kawai S, et al. Detection of ras gene mutations in pancreatic juice and peripheral blood of patients with pancreatic adenocarcinoma. Cancer Res 1993;53:2472–4.
29. Ohuchida K, Mizumoto K, Ishikawa N, et al. A highly sensitive and quantitative telomerase activity assay with pancreatic juice is useful for diagnosis of pancreatic carcinoma without problems due to polymerase chain reaction inhibitors: analysis of 100 samples of pancreatic juice from consecutive patients. Cancer 2004;101:2309–17.
30. Tada M, Ohashi M, Shiratori Y, et al. Analysis of K-ras gene mutation in hyperplastic duct cells of the pancreas without pancreatic disease. Gastroenterology 1996;110:227–31.
31. Ohuchida K, Mizumoto K, Yamada D, et al. Quantitative analysis of human telomerase reverse transcriptase in pancreatic cancer. Clin Cancer Res 2006; 12:2066–9.

ANTICANCER RESEARCH *27*: 793-800 (2007)

Increased Expression of *ADAM 9* and *ADAM 15* mRNA in Pancreatic Cancer

DAISUKE YAMADA, KENOKI OHUCHIDA, KAZUHIRO MIZUMOTO, SEIJI OHHASHI, JUN YU, TAKUYA EGAMI, HAYATO FUJITA, EISHI NAGAI and MASAO TANAKA

Department of Surgery and Oncology, Graduate School of Medical Sciences, Kyushu University, Fukuoka, Japan

Abstract. *Background: A disintegrin and metalloproteases (ADAMs) comprise a multifunctional family of membrane-anchored proteins. ADAM 9 and ADAM 15 are involved in cell migration and invasion. Expression of ADAM 9 and ADAM 15 was reported to be altered in several types of cancer. Materials and Methods: Quantitative real-time reverse transcription-polymerase chain reaction was performed to measure the expression of ADAM 9 mRNA in bulk pancreatic tissues. Results showed no significant difference in the expression of ADAM 9 mRNA between pancreatic cancer and non-neoplastic pancreas. Primary cultured pancreatic fibroblasts also expressed ADAM 9 mRNA. Therefore, a laser microdissection and pressure catapulting technique was employed to isolate cancer cells from tumor tissues. The expression of ADAM 9 and ADAM 15 mRNA was measured in microdissected samples (cancer cells, n=11; normal epithelial cells, n=13 for ADAM 9; cancer cells, n=9; normal epithelial cells, n=9 for ADAM 15). Results: Pancreatic cancer cells expressed significantly higher levels of ADAM 9 and ADAM 15 mRNA than did normal pancreatic epithelial cells (p=0.016 for ADAM 9; p=0.004 for ADAM 15). Conclusion: ADAM 9 and ADAM 15 are involved in pancreatic cancer. Microdissection-based analysis appears to be indispensable for the accurate analysis of the expression of certain ADAM family members in pancreatic cancer.*

Pancreatic cancer is one of the most lethal cancers with an overall 5-year survival rate after resection of approximately 10-20% (1). Despite improvements in chemotherapy and radiotherapy, the prognosis for pancreatic cancer has remained poor for decades because of its extremely aggressive nature. In order to improve the prognosis for pancreatic cancer, the identification of novel target genes for therapy is necessary.

Approximately 40 members have been identified of the family of multifunctional membrane-anchored proteins known as ADAMs (a disintegrin and metalloproteases). ADAMs are composed of a metalloprotease, a disintegrin, a cysteine-rich, an epidermal growth factor (EGF)-like, a transmembrane and a cytoplasmic domain (2). Each domain exerts its own unique functions. The metalloprotease domain cleaves the ectodomains of cytokines, growth factors, receptors and other molecules. The disintegrin domain binds integrins and is involved in cell-cell and cell-matrix interactions (3). Each ADAM exerts diverse functions according to the targets of the metalloprotease domain and the binding sites of the disintegrin domain.

ADAM 9 has been reported to be overexpressed in several cancers (4-9). Targets of the ADAM 9 metalloprotease domain are epidermal growth factor receptor (EGFR) ligands (10), and the disintegrin domain of ADAM 9 binds alfa(v)beta(5) (11), alfa(9)beta(1) (12) and alfa(6)beta(1) (13) integrins and degrades extracellular matrix (ECM) components including fibronectin and gelatin (12). On the basis of these functions, ADAM 9 is believed to be involved in malignancy. Many recent studies have suggested a relation between ADAM 9 and various cancers. ADAM 9 has been reported to be up-regulated in breast (4, 5) and prostate cancer (6) and has been associated with tumor aggressiveness and progression in liver (7) and non-small cell lung cancer (9). Gene expression profiling by microarray has suggested that *ADAM 9* is overexpressed in pancreatic cancer and its cell lines (14, 15). Immunohistochemistry has also suggested that ADAM 9 expression is associated with poor tumor differentiation and poor patient prognosis in pancreatic cancer (16).

ADAM15 has been reported to be dysregulated in several cancers (17-19). Targets of the ADAM 15 metalloprotease domain include amphiregulin, epiregulin (20) and CD23 (21). Amphiregulin and epiregulin constitute EGFR ligands. The disintegrin domain of ADAM 15 binds alfa(5)beta(1)

Correspondence to: Dr. K. Mizumoto, Department of Surgery and Oncology, Graduate School of Medical Sciences, Kyushu University, 3-1-1 Maidashi, Fukuoka 812-8582, Japan. Tel: +81 92 642 5440, Fax: +81 92 642 5458, e-mail: mizumoto@med.kyushu-u.ac.jp

Key Words: ADAM 9, ADAM 15, pancreatic cancer, microdissection, quantitative real-time RT-PCR.

(22), alfa(v)beta(3) (23) and alfa(9)beta(1) (24) integrins and degrades ECM components including Type IV collagen and gelatin (12). On the basis of these functions, *ADAM 15* is also thought to be involved in malignancy. ADAM 15 and ADAM 9 have been shown to be up-regulated in gastric cancer (17). ADAM 15 expression has also been reported to be associated with aggressive prostate and breast cancers (18). Schutz *et al.* (19) reported that ADAM 15 was frequently detected in lung carcinoma cell lines and tissues, and that lung cancer cells located at the invasion front expressed significantly higher levels of ADAM 15 than those located within the tumor center. To date, however, there have been no reports regarding the expression of ADAM 15 in pancreatic cancer.

In the present study, to clarify the involvement of ADAM 9 and ADAM 15 in pancreatic cancer, we investigated mRNA expression using one-step quantitative real-time reverse transcriptase-polymerase chain reaction (real-time RT-PCR).

Materials and Methods

Cultured cells and pancreatic tissues. The following 13 human pancreatic cancer cell lines were used: ASPC-1, BxPC-3, KP-1N, KP-2, Panc-1 and SUIT-2 (Dr. H. Iguchi, National Kyushu Cancer Center, Fukuoka, Japan); MIA PaCa-2 (Japanese Cancer Resource Bank, Tokyo, Japan); Capan-1, Capan-2, CFPAC-1, SW1990 and HS766T (American Type Culture Collection, Manassas, VA, USA), and NOR-P1 (established from a metastatic subcutaneous tumor of a patient with pancreatic cancer; 25). Six primary cultures of pancreatic fibroblasts derived from patients with invasive pancreatic adenocarcinoma were used in the present study. Cells were maintained as described elsewhere (26). Tissue samples were obtained during surgery at Kyushu University Hospital (Fukuoka, Japan) during the period February 15, 2001 to July 15, 2005, as described elsewhere (27). A total of 23 pancreatic cancer tissue samples were obtained from the primary tumor of each resected pancreas. The diagnosis of pancreatic cancer was confirmed by histological examination of resected specimens. Twelve non-neoplastic pancreata were obtained away from the pancreatic tumor or were normal pancreata resected due to cholangiocarcinoma, as described elsewhere (27). Experienced pathologists performed histological examination of all tissues adjacent to the specimens. Written informed consent was obtained from all patients and the study was approved by our institution's surveillance committee and conducted according to the Helsinki Declaration.

Isolation of total RNA. Total RNA was extracted according to the standard acid guanidinium thiocyanate phenol chloroform protocol (28), with glycogen (Funakoshi, Tokyo, Japan). Pancreatic cancer cells and normal pancreatic epithelial cells were isolated from frozen sections using a laser microdissection and pressure catapulting system (LMPC) and then extracted total RNA from these isolated cells. RNA extracts were measured with a NanoDrop ND-1000 spectrophotometer (NanoDrop Technologies, Inc., Rockland, DE, USA), at 260 nm and 280 nm. RNA integrity was assessed with an Agilent Bioanalyzer 2100 (Agilent Technologies, Palo Alto, CA, USA).

Quantitative analysis of ADAM 9 and ADAM 15 mRNA levels via one-step real-time RT-PCR with gene-specific primers. One-step quantitative real-time RT-PCR was used with gene-specific primers to examine mRNA levels of *ADAM 9* and *ADAM 15*. We designed specific primers (ADAM 9 forward: 5'-gttcctgtggagcaaagagc-3', reverse: 5'-ccagcgtccaccaacttatt-3'; ADAM 15 forward: 5'-agcctcaaaaaggtgcttca-3', reverse: 5'-ccctggtagcagcagttctc-3'; 185 rRNA forward: 5'-ccatccaatcggtagtagcg-3', reverse: 5'-gtaacccgttgaaccccatt-3') BLAST searches to ensure the specificity of these primers. One-step quantitative real-time RT-PCR with gene-specific primers was performed with a QuantiTect SYBR Green RT-PCR Kit (Qiagen K.K., Tokyo, Japan) and a LightCycler Quick System 350S (Roche Diagnostics K.K., Tokyo, Japan). The reaction mixture was incubated at 50°C for 20 min to allow for reverse transcription, during which first-strand cDNA was synthesized by priming with a gene-specific primer. PCR was initiated with one cycle of 95°C for 15 min to activate modified Taq polymerase followed by 40 cycles of 94°C for 15 sec, 55°C for 25 sec and 72°C for 10 sec, followed by one cycle of 95°C for 0 sec, 65°C for 15 sec and +0.1°C/s to 95°C for melting analysis to visualize nonspecific PCR products, different fragments showed separate distinct melting peaks. Each primer set used in the present study produced a single melting peak and a single prominent band of expected size on microchip electrophoresis. Each sample was run twice and any sample showing greater than 10% deviation from the RT-PCR value was tested a third time. Levels of mRNA in each sample were calculated from a standard curve generated with total RNA from Capan-1 human pancreatic cancer cells. Levels of *ADAM 9* and *ADAM 15* mRNA were normalized to that of *18S rRNA*. Samples were used that showed ADAM levels greater than the levels of *18S rRNA* corresponding to 0.05 ng of total RNA derived from Capan-1 cells. When levels of *ADAM 9* or *ADAM 15* mRNA were not detected due to the limitation of our real-time RT-PCR-based assay (the level corresponding to 0.01 ng of total RNA derived from Capan-1 cells), expression values were defined as this level.

Microdissection-based quantitative analysis of ADAM 9 and ADAM 15 mRNA. Frozen tissue samples were cut into 8-μm-thick sections. One section was stained with hematoxylin and eosin (H&E) for histological examination. We used a laser microdissection and pressure catapulting system (LMPC; PALM MicroLaser Technologies AG, Bernried, Germany), according to the manufacturer's instructions to selectively isolate pancreatic cancer cells from 11 sections and normal pancreatic epithelial cells from 13 sections for quantification of *ADAM 9* mRNA, and pancreatic cancer cells from 9 sections and normal pancreatic epithelial cells from 9 sections for quantification of *ADAM 15* mRNA. After microdissection, total RNA was extracted from the isolated cells and was subjected to one-step real-time RT-PCR for quantitative measurement of *ADAM 9* or *ADAM 15* mRNA.

Statistical analysis. Data were analyzed using the Mann-Whitney *U*-test because the data did not follow a normal distribution. Statistical significance was set at $p<0.05$.

Results

Quantitative analysis of ADAM 9 mRNA expression in bulk tissues of pancreatic cancer and non-neoplastic pancreas. ADAM 9 mRNA expression did not differ significantly between bulk tissues of pancreatic cancer and non-

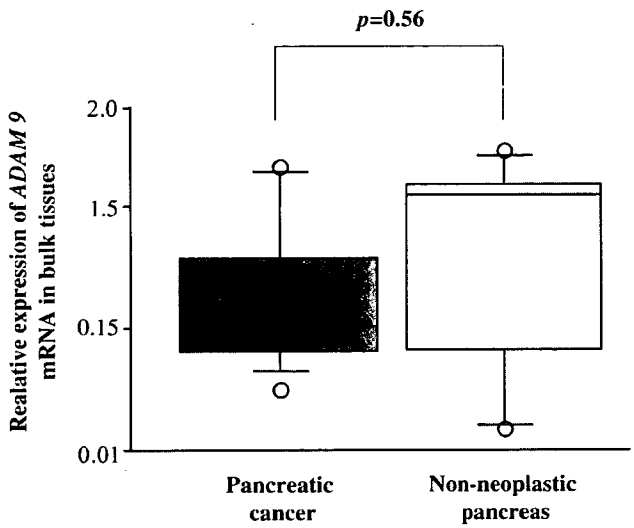

Figure 1. *Quantitative analysis of ADAM 9 mRNA expression in bulk tissues of pancreatic cancer and non-neoplastic pancreas. Expression of ADAM 9 mRNA was measured using one-step quantitative real-time RT-PCR with gene-specific primers and was normalized to that of 18S rRNA. Expression of ADAM 9 mRNA did not differ significantly between bulk tissues of pancreatic cancer and non-neoplastic pancreas (p=0.56).*

neoplastic pancreas (Figure 1, $p=0.56$). Pancreatic cancer tissues typically contain a few carcinoma cells amid a large amount of other structures such as stromal components composed of fibroblasts, endothelial cells and inflammatory cells. Non-neoplastic pancreata included in the present study were typically taken from the distal normal portion of resected pancreata with pancreatic tumors. The histological appearance of these non-neoplastic pancreata showed chronic pancreatitis, possibly secondary pancreatitis due to the occlusion of pancreatic ducts by tumor. These pancreata were also typically composed of various components including inflammatory lesions, stromal lesions and remnant normal structures. These findings suggest that analysis of bulk tissues does not accurately reflect expression levels of *ADAM 9* mRNA in pancreatic cancer cells and normal pancreatic epithelial cells.

Quantitative analysis of ADAM 9 and ADAM 15 mRNA expression in human pancreatic cancer cell lines and primary cultures of pancreatic fibroblasts. The present bulk tissue analysis showed no significant difference in the level of *ADAM 9* mRNA between bulk tissues of pancreatic cancer and non-neoplastic pancreas. We performed histological examination of these tissues and found that most of the pancreatic cancer samples and a subset of the non-neoplastic pancreas samples consisted predominantly of stromal components. In order to evaluate the effect of stromal cells in these tissues on *ADAM 9* and *ADAM 15* mRNA expression, we measured *ADAM 9* and *ADAM 15* mRNA in primary cultures of pancreatic fibroblasts and compared these levels with those in cultured pancreatic cancer cell lines.

Primary cultures of pancreatic fibroblasts showed levels of *ADAM 9* mRNA similar to those of pancreatic cancer cell lines (Figure 2A). These results suggest that the presence of fibroblasts in bulk tissues may affect the expression profiles of *ADAM 9* mRNA in cancer. Pancreatic cancer cell lines also showed significant levels of *ADAM 9* mRNA, but we found no correlation between the histological grade of differentiation and the level of *ADAM 9* mRNA.

The levels of *ADAM 15* mRNA in primary cultures of pancreatic fibroblasts were much lower than those in pancreatic cancer cell lines (Figure 2B). All of the pancreatic cancer cell lines examined in the present study expressed significant levels of *ADAM 15* mRNA, but we found no correlation between the histological grade of differentiation and the level of *ADAM 15* mRNA.

Quantitative analysis of ADAM 9 and ADAM 15 mRNA expression in microdissected pancreatic cancer cells and normal pancreatic epithelial cells. On the basis of the results obtained with bulk tissues and cultured cells, we performed LMPC to isolate pancreatic cancer cells and normal pancreatic epithelial cells so as to obtain accurate *ADAM 9* and *ADAM 15* mRNA expression profiles. We then measured *ADAM 9* and *ADAM 15* mRNA expression in these cells with one-step quantitative real-time RT-PCR with gene-specific primers. We typically isolated pancreatic cancer cells from invasive components of pancreatic cancer tissues and normal epithelial cells from normal pancreata or chronic pancreatitis-affected pancreata. Microdissected pancreatic cancer cells showed significantly higher levels of *ADAM 9* mRNA (median, 1.79) than did normal pancreatic epithelial cells (median, 0.85; $p=0.016$) (Figure 3A). Similarly, microdissected pancreatic cancer cells showed significantly higher levels of *ADAM 15* mRNA (median, 0.12) than did normal pancreatic epithelial cells (median, 0.02; $p=0.004$) (Figure 3B). We found no correlation between the histological grade of differentiation and the level of *ADAM 9* or *ADAM 15* mRNA in microdissected pancreatic cancer cells, similar to the results obtained with pancreatic cancer cell lines (Figure 2A).

We measured both *ADAM 9* and *ADAM 15* mRNA in seven microdissected samples of pancreatic cancer cells. We found no significant correlation between *ADAM 9* and *ADAM 15* mRNA levels. None of the samples showed high levels of both *ADAM 9* and *ADAM 15* mRNA. Two of the seven samples of pancreatic cancer cells (28.5%) showed low levels of both *ADAM 9* and *ADAM 15* mRNA. Five of the seven samples (71.5%) showed significant levels of *ADAM 9* or *ADAM 15* mRNA. These results suggest that *ADAM 9* and *ADAM 15* may play independent roles in pancreatic cancer.

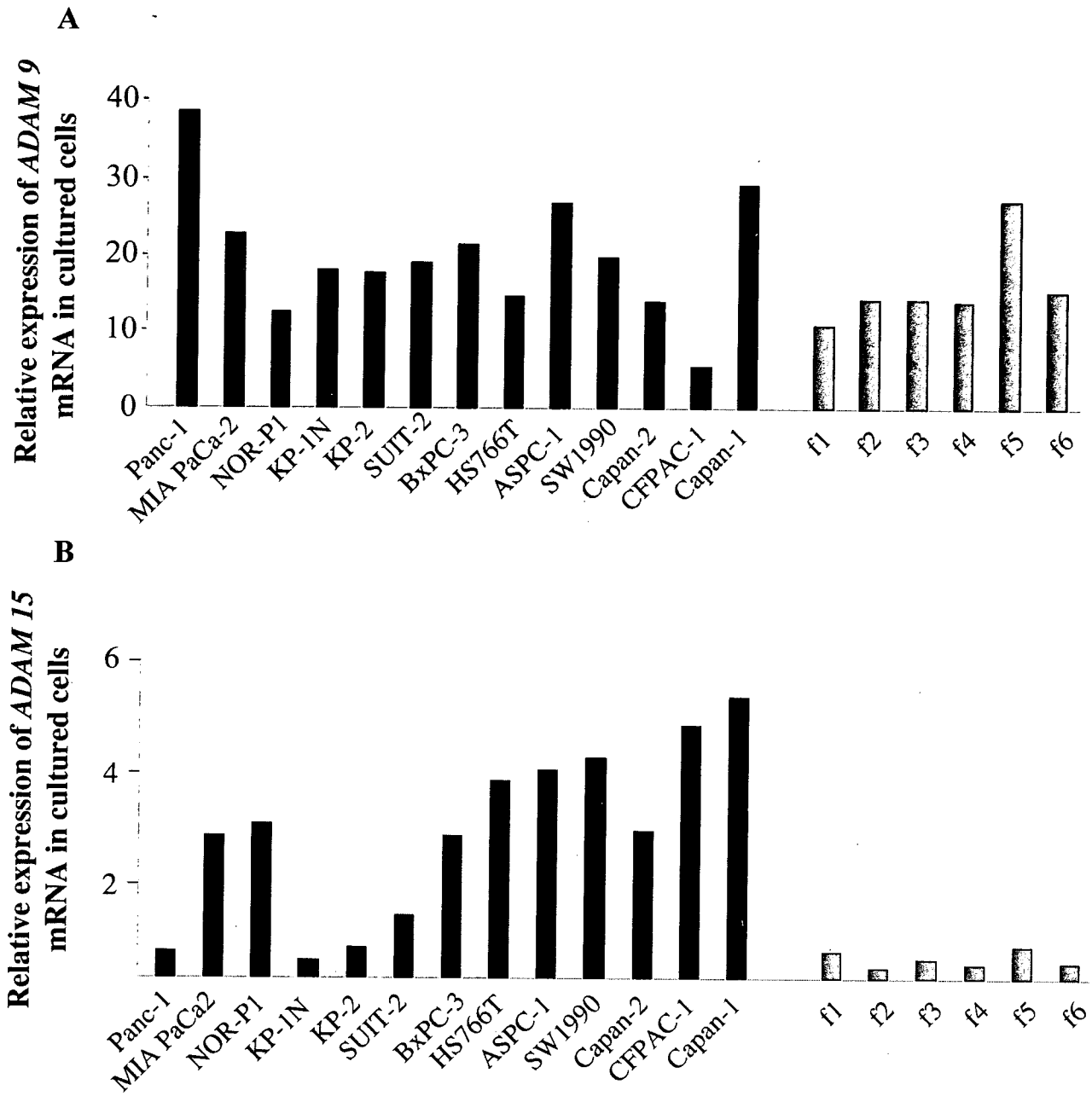

Figure 2. *Quantitative analysis of ADAM 9 and ADAM 15 mRNA expression in human pancreatic cancer cell lines (Panc-1 to Capan-1) and primary cultured pancreatic fibroblast (f1-f6). We measured ADAM 9 and ADAM15 mRNA expression in 13 pancreatic cancer cell lines and six cultures of primary cultured pancreatic fibroblast. All of the pancreatic cancer cell lines and the primary cultured pancreatic fibroblasts expressed ADAM 9 and ADAM 15 mRNA. We found no correlation between the histological grade of differentiation and levels of ADAM 9 and ADAM 15 mRNA in cultured pancreatic cancer cells. Primary cultured pancreatic fibroblasts showed levels of ADAM 9 mRNA similar to those of the pancreatic cancer cell lines, but the levels of ADAM 15 mRNA were much lower in primary cultured pancreatic fibroblasts than in pancreatic cancer cell lines.*

Five out of nine samples of normal pancreatic epithelial cells (55.6%) showed *ADAM 15* mRNA levels below the level corresponding to 0.01 ng of total RNA derived from Capan-1 cells, although these cells showed higher levels of *18S rRNA* than the levels corresponding to 0.08 ng of total RNA derived from Capan-1 cells, suggesting that the relative levels of *ADAM 15* mRNA normalized to the levels of *18S rRNA* in these samples were lower than 0.125, which was used as the

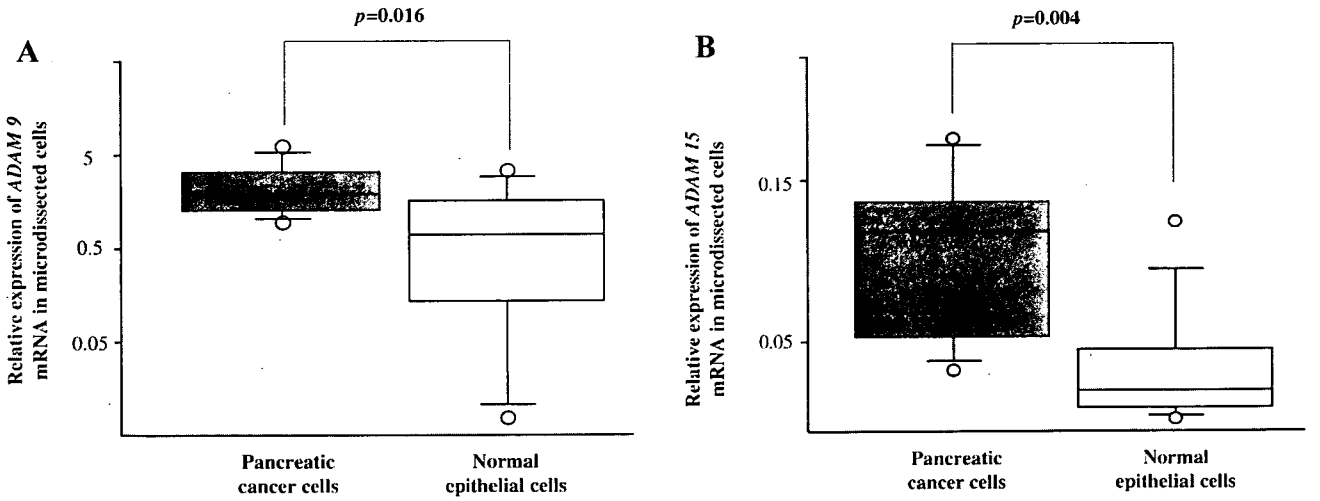

Figure 3. *Quantitative analysis of ADAM 9 and ADAM 15 mRNA in pancreatic cancer cells and normal pancreatic epithelial cells. We isolated pancreatic cancer cells and normal pancreatic epithelial cells from frozen sections by microdissection and performed one-step quantitative real-time RT-PCR with gene-specific primers to analyze the levels of ADAM 9 and ADAM 15 mRNA in these cells. Expression of ADAM 9 and ADAM 15 mRNA was normalized to that of 18S rRNA. We found that pancreatic cancer cells showed significantly higher levels of ADAM 9 and ADAM 15 mRNA than did normal pancreatic epithelial cells (p=0.016 for ADAM 9; p=0.004 for ADAM 15).*

value for statistical analysis. In contrast, 9 out of 13 samples of normal pancreatic epithelial cells (79.2%) showed significant levels of *ADAM 9* mRNA. In the present study, cultured pancreatic fibroblasts showed significant levels of *ADAM 9* mRNA but did not show any *ADAM 15* mRNA. These results suggest that *ADAM 15* may not play a major role under normal conditions and may not be involved in tumor-stromal cell interactions; expression of *ADAM 15* may be more specific than that *ADAM 9* to pancreatic cancer cells.

In the present microdissection-based experiments, 8 out of 11 samples (72.7%) were derived from resected tumors with lymph node metastasis. Levels of *ADAM 9* mRNA in these 8 samples (median, 2.17) were higher than those in the samples without lymph node metastasis (median, 1.07), although the difference was not statistically significant ($p=0.07$). Seven out of 11 patients included in the present study (63.6%) survived longer than 15 months, and the levels of *ADAM 9* mRNA in the samples from these patients (median, 1.31) were lower than those in the other samples (median, 2.38), although the difference was not statistically significant ($p=0.06$). These results are consistent with previous reports suggesting that ADAM 9 may play roles in tumor aggressiveness, progression and prognosis (8, 16).

Discussion

In this study, we performed quantitative analysis of *ADAM 9* and *ADAM 15* mRNA levels in human pancreatic cancer cell lines, primary cultured pancreatic fibroblasts, microdissected pancreatic cancer cells and normal pancreatic epithelial cells with quantitative real-time RT-PCR. Analysis of bulk tissues showed no significant difference in the levels of *ADAM 9* mRNA between pancreatic cancer and non-neoplastic pancreas. However, using microdissection we found that pancreatic cancer cells showed significantly higher levels of *ADAM 9* mRNA than did normal epithelial cells. Pancreatic cancer tissues typically contain a few ductal carcinoma cells amid a large amount of stromal components. We also confirmed that primary cultured pancreatic fibroblasts express significant levels of *ADAM 9* mRNA. Grutzmann *et al.* (14) performed microdissection and microarray based gene expression analysis and found differential expression of *ADAM 9* between pancreatic cancer cells and normal epithelial cells. However, Tan *et al.* (29) reported no overexpression of *ADAM 9* using microarray analysis of bulk pancreatic cancer tissues. Thus, microdissection is necessary for the accurate analysis of *ADAM 9* in pancreatic cancer.

All of the primary cultured pancreatic fibroblasts analyzed expressed *ADAM 9* and *ADAM 15* mRNA. Levels of *ADAM 9* mRNA were similar to those of cultured pancreatic cancer cell lines. Mazzocca *et al.* (30) reported that ADAM 9 protein was expressed by stromal liver myofibroblasts in metastatic liver tumors and suggested that ADAM 9 secreted by stromal liver myofibroblasts may promote carcinoma invasion. Primary cultured pancreatic fibroblasts examined in the present study were obtained from tumors with the histological appearance of invasive ductal carcinoma, indicating that tumor-associated

pancreatic fibroblasts may play an important role in the progression of pancreatic cancer. However, *ADAM 15* may not be involved in tumor-stromal cell interactions because the expression levels of *ADAM 15* mRNA in primary cultures of pancreatic fibroblasts were much lower than those in cultured pancreatic cancer cell lines.

In the present study, we isolated pancreatic cancer cells from tumors for microdissection-based quantitative analysis. Results showed that the levels of *ADAM 9* mRNA were significantly higher in pancreatic cancer cells than in normal epithelial cells. In addition, the levels of *ADAM 9* mRNA appeared to be related to lymph node metastasis and prognosis. ADAM 9 sheds and activates several growth factors, such as heparin-binding EGF and transforming growth factor-alpfa (10), and also binds several integrins (11-13) and degrades ECM components such as fibronectin and gelatin (12). Mazzocca *et al.* (30) showed that ADAM 9 promotes carcinoma invasion, suggesting that ADAM 9 plays a role in pancreatic cancer, contributing to its aggressiveness and poor prognosis.

Microdissection-based quantitative analysis showed that the levels of *ADAM 15* mRNA were significantly higher in pancreatic cancer cells than in normal epithelial cells. The targets of ADAM 15 ectodomain shedding are EGF family ligands (20). The disintegrin domain of ADAM 15 binds several integrins (22-24) and degrades ECM components such as Type IV collagen and gelatin (12). ADAM 15 has been reported to be up-regulated in malignant tumors and related to tumor aggressiveness (17-19). However, Herren *et al.* (31) reported that ADAM 15 overexpression enhanced cell-cell interactions and reduced cell migration. The role of ADAM 15 in cancer progression remains controversial. Our results showed that *ADAM 15* mRNA was up-regulated in pancreatic cancer, suggesting that ADAM 15 may play a role in the progression of pancreatic cancer. However, we found no relation between the level of *ADAM 15* mRNA and the status of lymph node metastasis, prognosis or histological differentiation, possibly due to the small number of samples analyzed. In the present study, levels of *ADAM 15* mRNA were much lower in primary cultured pancreatic fibroblasts than in pancreatic cancer cell lines. Microdissection-based analysis showed that normal pancreatic epithelial cells expressed extremely low levels of *ADAM 15* mRNA but significant levels of *ADAM 9* mRNA, suggesting that the expression of ADAM 15 may be more specific than the expression of ADAM 9 to pancreatic cancer cells.

Conclusion

We confirmed upregulation of *ADAM 9* and *ADAM 15* mRNA expression in microdissected pancreatic cancer cells and found that LMPC is indispensable for the accurate analysis of these genes in pancreatic cancer. *ADAM 9* and *ADAM 15* may play roles in the progression of pancreatic cancer and may present promising target genes for the diagnosis and treatment of pancreatic cancer.

References

1 Yeo CJ, Abrams RA, Grochow LB *et al*: Pancreaticoduodenectomy for pancreatic adenocarcinoma: postoperative adjuvant chemoradiation improves survival. A prospective, single-institution experience. Ann Surg *225*: 621-633; discussion 633-636, 1997.

2 Seals DF and Courtneidge SA: The ADAMs family of metalloproteases: multidomain proteins with multiple functions. Genes Dev *17*: 7-30, 2003.

3 Blobel CP *et al*: ADAMs: key components in EGFR signalling and development. Nat Rev Mol Cell Biol *6*: 32-43, 2005.

4 Lendeckel U, Kohl J, Arndt M *et al*: Increased expression of ADAM family members in human breast cancer and breast cancer cell lines. J Cancer Res Clin Oncol *131*: 41-48, 2005.

5 O'Shea C, McKie N, Buggy Y *et al*: Expression of ADAM-9 mRNA and protein in human breast cancer. Int J Cancer *105*: 754-761, 2003.

6 Karan D, Lin FC, Bryan M *et al*: Expression of ADAMs (a disintegrin and metalloproteases) and TIMP-3 (tissue inhibitor of metalloproteinase-3) in human prostatic adenocarcinomas. Int J Oncol *23*: 1365-1371, 2003.

7 Tannapfel A, Anhalt K, Hausermann P *et al*: Identification of novel proteins associated with hepatocellular carcinomas using protein microarrays. J Pathol *201*: 238-249, 2003.

8 Le Pabic H, Bonnier D, Wewer UM *et al*: ADAM12 in human liver cancers: TGF-beta-regulated expression in stellate cells is associated with matrix remodeling. Hepatology *37*: 1056-1066, 2003.

9 Shintani Y, Higashiyama S, Ohta M *et al*: Overexpression of ADAM9 in non-small cell lung cancer correlates with brain metastasis. Cancer Res *64*: 4190-4196, 2004.

10 Peduto L, Reuter VE, Shaffer DR *et al*: Critical function for ADAM9 in mouse prostate cancer. Cancer Res *65*: 9312-9319, 2005.

11 Zhou M, Graham R, Russell G *et al*: MDC-9 (ADAM-9/Meltrin gamma) functions as an adhesion molecule by binding the alpha(v)beta(5) integrin. Biochem Biophys Res Commun *280*: 574-580, 2001.

12 White JM: ADAMs: modulators of cell-cell and cell-matrix interactions. Curr Opin Cell Biol *15*: 598-606, 2003

13 Nath D, Slocombe PM, Webster A *et al*: Meltrin gamma (ADAM-9) mediates cellular adhesion through alpha(6)beta(1) integrin, leading to a marked induction of fibroblast cell motility. J Cell Sci *113(Pt 12)*: 2319-2328, 2000.

14 Grutzmann R, Foerder M, Alldinger I *et al*: Gene expression profiles of microdissected pancreatic ductal adenocarcinoma. Virchows Arch *443*: 508-517, 2003.

15 Alldinger I, Dittert D, Peiper M *et al*: Gene expression analysis of pancreatic cell lines reveals genes overexpressed in pancreatic cancer. Pancreatology *5*: 370-379, 2005.

16 Grutzmann R, Luttges J, Sipos B *et al*: ADAM9 expression in pancreatic cancer is associated with tumour type and is a prognostic factor in ductal adenocarcinoma. Br J Cancer *90*: 1053-1058, 2004.

17 Carl-McGrath S, Lendeckel U, Ebert M *et al*: The disintegrin-metalloproteinases ADAM9, ADAM12, and ADAM15 are upregulated in gastric cancer. Int J Oncol *26*: 17-24, 2005.
18 Kuefer R, Day KC, Kleer CG *et al*: ADAM15 disintegrin is associated with aggressive prostate and breast cancer disease. Neoplasia *8*: 319-329, 2006.
19 Schutz A, Hartig W, Wobus M *et al*: Expression of ADAM15 in lung carcinomas. Virchows Arch *446*: 421-429, 2005.
20 Sahin U, Weskamp G, Kelly K *et al*: Distinct roles for ADAM10 and ADAM17 in ectodomain shedding of six EGFR ligands. J Cell Biol *164*: 769-779, 2004.
21 Fourie AM, Coles F, Moreno V *et al*: Catalytic activity of ADAM8, ADAM15, and MDC-L (ADAM28) on synthetic peptide substrates and in ectodomain cleavage of CD23. J Biol Chem *278*: 30469-30477, 2003.
22 Nath D, Slocombe PM, Stephens PE *et al*: Interaction of metargidin (ADAM-15) with alphavbeta3 and alpha5beta1 integrins on different haemopoietic cells. J Cell Sci *112(Pt 4)*: 579-587, 1999.
23 Zhang XP, Kamata T, Yokoyama K *et al*: Specific interaction of the recombinant disintegrin-like domain of MDC-15 (metargidin, ADAM-15) with integrin alphavbeta3. J Biol Chem *273*: 7345-7350, 1998.
24 Eto K, Puzon-McLaughlin W, Sheppard D *et al*: RGD-independent binding of integrin alpha9beta1 to the ADAM-12 and -15 disintegrin domains mediates cell-cell interaction. J Biol Chem *275*: 34922-34930, 2000.
25 Sato N, Mizumoto K, Beppu K *et al*: Establishment of a new human pancreatic cancer cell line, NOR-P1, with high angiogenic activity and metastatic potential. Cancer Lett *155*: 153-161, 2000.
26 Ohuchida K, Mizumoto K, Murakami M *et al*: Radiation to stromal fibroblasts increases invasiveness of pancreatic cancer cells through tumor-stromal interactions. Cancer Res *64*: 3215-3222, 2004.
27 Ohuchida K, Mizumoto K, Yamada D *et al*: Quantitative analysis of MUC1 and MUC5AC mRNA in pancreatic juice for preoperative diagnosis of pancreatic cancer. Int J Cancer *118*: 405-411, 2006.
28 Tachikawa T and Irie T: A new molecular biology approach in morphology: basic method and application of laser microdissection. Med Electron Microsc *37*: 82-88, 2004.
29 Tan ZJ, Hu XG, Cao GS *et al*: Analysis of gene expression profile of pancreatic carcinoma using cDNA microarray. World J Gastroenterol *9*: 818-823, 2003.
30 Mazzocca A, Coppari R, De Franco R *et al*: A secreted form of ADAM9 promotes carcinoma invasion through tumor-stromal interactions. Cancer Res *65*: 4728-4738, 2005.
31 Herren B, Garton KJ, Coats S *et al*: ADAM15 overexpression in NIH3T3 cells enhances cell-cell interactions. Exp Cell Res *271*: 152-160, 2001.

Received October 30, 2006
Accepted December 29, 2006

The Role of the DNA Damage Checkpoint Pathway in Intraductal Papillary Mucinous Neoplasms of the Pancreas

Yoshihiro Miyasaka,[1] Eishi Nagai,[2] Hiroshi Yamaguchi,[1] Kei Fujii,[1] Takahiro Inoue,[1] Kenoki Ohuchida,[2] Tomomi Yamada,[3] Kazuhiro Mizumoto,[2] Masao Tanaka,[2] and Masazumi Tsuneyoshi[1]

Abstract

Purpose: Intraductal papillary mucinous neoplasms (IPMN) are known to show a transition from adenoma to carcinoma accompanied by several molecular abnormalities. ATM-Chk2-p53 DNA damage checkpoint activation, which is involved in prevention of the progression of several tumors, was analyzed to evaluate the role of the DNA damage checkpoint in the progression of IPMNs.

Experimental Design: One hundred and twenty-eight IPMNs were classified into four groups (intraductal papillary mucinous adenoma, borderline IPMN, noninvasive intraductal papillary mucinous carcinoma, and invasive intraductal papillary mucinous carcinoma) and stained immunohistochemically using antibody for Thr^{68}-phosphorylated Chk2. Expression of ATM, Chk2, and $p21^{WAF1}$ and accumulation of p53 were also analyzed.

Results: Chk2 phosphorylation was shown in all adenomas and showed a significant decreasing trend with the progression of atypia ($P < 0.0001$ by the Cochran-Armitage test for trend). Expression of $p21^{WAF1}$ also exhibited a decreasing tendency ($P < 0.0001$), reflecting DNA damage checkpoint inactivation. p53 accumulation was mostly detected in malignant IPMNs. It was suggested that the DNA damage checkpoint provides a selective pressure for p53 mutation.

Conclusion: Our findings indicate that DNA damage checkpoint activation occurs in the early stage of IPMNs and prevents their progression. It is suggested that disturbance of the DNA damage checkpoint pathway due to Chk2 inactivation or p53 mutation contributes to the carcinogenesis of IPMNs.

Intraductal papillary mucinous neoplasms (IPMN) are pancreatic exocrine tumors composed of dilated main or branch ducts lined by mucin-producing atypical epithelium, which usually proliferates in a papillary fashion (Fig. 1; refs. 1, 2). Based on their architectural and nuclear atypia, the WHO has divided IPMNs into three groups: intraductal papillary mucinous adenoma (IPMA), borderline IPMN (IPMB), and intraductal papillary mucinous carcinoma (IPMC; ref. 1). Borderline lesions and carcinoma are accompanied by less atypical lesions in the vicinity, and transition from adenoma to adenocarcinoma is recognized within lesions. They are considered to exhibit a pattern of progression similar to that seen in colorectal adenocarcinoma [i.e., the adenoma-carcinoma sequence (3, 4)]. Some IPMCs are restricted to epithelium, whereas others are associated with invasive carcinoma. Sohn et al. (5) investigated 136 patients with IPMNs, including 52 with invasive carcinoma, and concluded that associated invasive carcinoma is the strongest prognostic factor.

Various biological changes associated with the progression of IPMNs have been reported. Biankin et al. (6) reported that the frequency of loss of $p16^{INK4A}$ and Smad4, cyclin D1 overexpression, and p53 accumulation are greater in IPMC and in IPMC with invasive carcinoma. House et al. (7) indicated that IPMNs with invasion tend to have multiple methylated genes, which are related to cell cycle control (*p16*, *p73*, and *APC*), DNA repair (*MGMT* and *hMLH1*), and cell adhesion (*E-cadherin*).

Recently, the DNA damage checkpoint pathway, including the ATM-Chk2-p53 pathway, was reported to be involved in tumorigenesis. The ATM-Chk2 pathway was originally shown to be activated in response to double-strand DNA breaks caused by ionizing radiation (8, 9). Responding to DNA damage, ATM phosphorylates Chk2 at Thr^{68}, and activated Chk2 phosphorylates downstream proteins, such as p53, activation of which leads to cell cycle arrest and DNA repair or apoptosis (Fig. 2). Bartkova et al. (10) showed that Chk2 phosphorylation occurred in colon adenoma and the early stage of urinary bladder cancer and decreased in advanced carcinoma. They thus suggested that the ATM-Chk2 DNA damage signaling pathway was activated and delayed or prevented tumor progression in the early stage of tumorigenesis. Gorgoulis et al. (11) reported the activation of the DNA damage checkpoint in precancerous lesions of lung and skin as

Authors' Affiliations: Departments of [1]Anatomic Pathology and [2]Surgery and Oncology, Graduate School of Medical Sciences, Kyushu University and [3]Department of Medical Information Science, Kyushu University Hospital, Fukuoka, Japan

Received 1/5/07; revised 4/9/07; accepted 5/11/07.

The costs of publication of this article were defrayed in part by the payment of page charges. This article must therefore be hereby marked *advertisement* in accordance with 18 U.S.C. Section 1734 solely to indicate this fact.

Requests for reprints: Masazumi Tsuneyoshi, Department of Anatomic Pathology, Graduate School of Medical Sciences, Kyushu University, 3-1-1 Maidashi, Higashi-ku, Fukuoka 812-8582, Japan. Phone: 81-92-642-6061; Fax: 81-92-642-5968; E-mail: masazumi@surgpath.med.kyushu-u.ac.jp.

doi:10.1158/1078-0432.CCR-07-0032

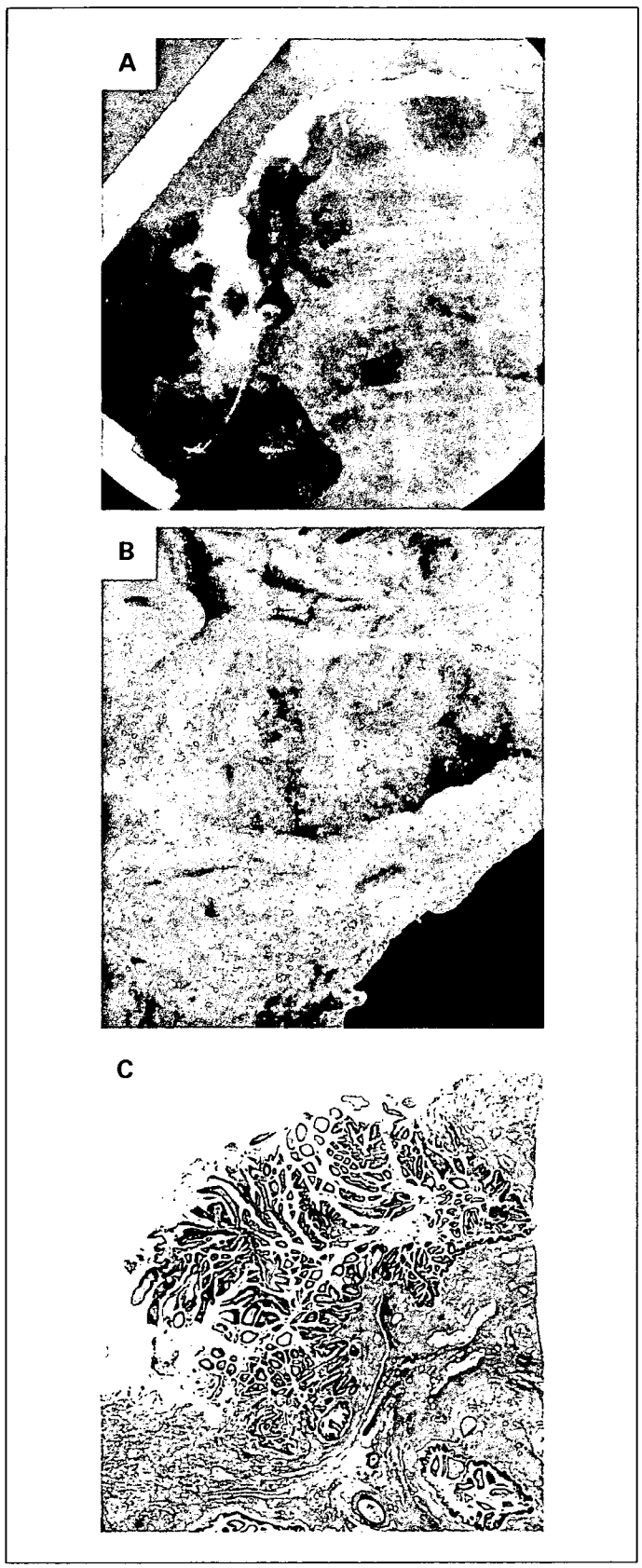

Fig. 1. *A* to *C*, a case of main duct type IPMN. *A*, endoscopic retrograde pancreatography visualizing dilated main pancreatic duct and nodules. *B*, pancreatoduodenectomy specimen with dilated main pancreatic duct containing multiple nodules. *C*, photomicrograph showing epithelial papillary projection on the main pancreatic duct wall. The histopathologic diagnosis was noninvasive IPMC.

indicated by phosphorylation of Chk2 and H2AX. It is proposed that frequent inactivation of p53 in carcinomas supports DNA damage checkpoint activation in precursor lesions because activated checkpoint might confer a selective pressure for p53 dysfunction (11, 12). Indeed, aberrations of checkpoint-related genes, such as *ATM*, *Chk2*, and *p53*, have been reported in the literature and their role as tumor suppressors has been widely accepted (13, 14). However, the role of the DNA damage checkpoint pathway in pancreatic neoplasms has not yet been investigated.

The existence of IPMNs with the adenoma-carcinoma sequence prompted us to investigate the status of the DNA damage checkpoint pathway in a large series of IPMNs. Activation of the pathway was evaluated by immunohistochemistry using antibody for Thr^{68}-phosphorylated Chk2. We also investigated expression of ATM, Chk2, and $p21^{WAF1}$, which is known as a downstream effector of the ATM-Chk2-p53 pathway, and accumulation of p53. The purpose of this study was to clarify the involvement of the DNA damage checkpoint pathway in the tumorigenesis and progression of IPMNs.

Materials and Methods

Tissue samples. One hundred and twenty-eight cases of IPMN were collected from the files of the Department of Anatomic Pathology of Kyushu University. All samples were obtained by surgery between July 1986 and January 2006. The original H&E slides for each case were reviewed by three pathologists (Y.M., T.I., and M.T.) independently, and the IPMNs were classified into four groups (IPMA, IPMB, noninvasive IPMC, or invasive IPMC) according to the WHO criteria (1). Because of the heterogeneity of the atypia in IPMN, we determined which lesion had the highest degree of architectural and cellar atypia in each case and selected it as a representative section. Normal ductal epithelia in these pancreata, which were available in 119 cases, were also evaluated.

Immunohistochemistry. Serial 3-μm sections were prepared from the selected paraffin blocks, deparaffinized in xylene, and rehydrated in ethanol. Endogenous peroxidase was blocked using 3% hydrogen peroxide in methanol for 30 min. Antigen retrieval was achieved by microwave in citrate buffer at pH 6.0. A Histofine SAB-PO kit (Nichirei) was used for immunohistochemical labeling. Each section was exposed to 10% nonimmunized rabbit serum (Chk2, ATM, p53, and $p21^{WAF1}$) or goat serum (phospho-Chk2) for 10 min to block nonspecific binding of the antibodies and then incubated with primary antibodies at 4°C overnight. We used the following antibodies obtained from commercial suppliers: rabbit monoclonal anti-phospho-Chk2 (Thr^{68}) antibody (80F5, 1:200; Cell Signaling), mouse monoclonal anti-Chk2 antibody (DCS-270, 1:200; MBL), mouse monoclonal anti-ATM antibody (ATX08, 1:50; Novus Biologicals), mouse monoclonal anti-p53 (PAb1801, 1:100; Oncogene), and mouse monoclonal anti-$p21^{WAF1}$ (EA10, 1:200; Calbiochem). The sections were conjugated with biotinylated anti-rabbit (phospho-Chk2) or anti-mouse (Chk2, ATM, p53, and $p21^{WAF1}$) immunoglobulin solution for 20 min followed by 20-min incubation with peroxidase-labeled streptavidin. For visualization of the reaction products, 3,3′-diaminobenzidine was used as a chromogen, and then nuclear counterstaining with hematoxylin was done.

Evaluation. Immunohistochemical staining was assessed by the three pathologists independently. To assess the expression of Chk2 and phospo-Chk2, we used the scoring system described by Eymin et al. (15). Scores were calculated by multiplying the percentage of positive cells (0-100) by the intensity score (0-3); when the score was ≥10, the tumor was considered positive for the antibody. Based on published reports, the criteria for staining with other antibodies were as follows: ≥5% nuclear and cytoplasmic staining was considered positive for ATM

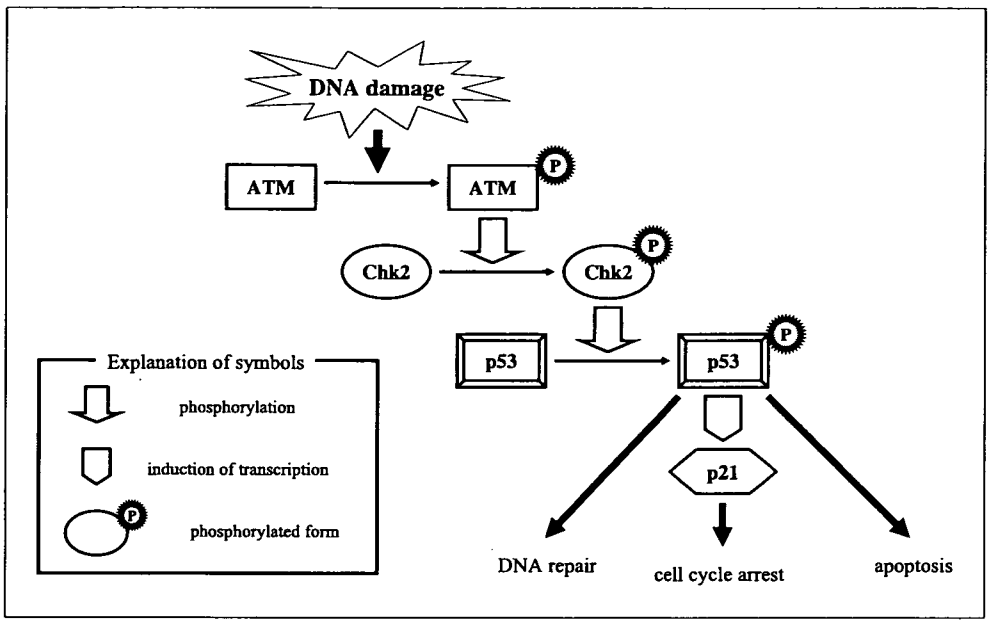

Fig. 2. Schema of the ATM-Chk2-p53 DNA damage checkpoint pathway. In response to DNA damage, activated ATM phosphorylates Chk2 at Thr^{68}. Activated Chk2, in turn, phosphorylates p53. Activated p53 induces transcription of downstream proteins, such as p21, which results in cell cycle arrest, DNA repair, and apoptosis.

(16) and ≥10% nuclear staining was considered positive for $p21^{WAF1}$ (17) or p53 accumulation (6).

Statistical analysis. Clinicopathologic characteristics were compared among the four groups using the χ^2 test, Fisher's exact test, or ANOVA with Bonferroni correction. The Cochran-Armitage test was used to determine trends of immunohistochemical staining. All analyses were done using Statistical Analysis System for Windows, release 8.2 (SAS Institute, Inc.).

Results

Clinicopathologic data. The 128 IPMNs analyzed in this study comprised 46 IPMAs, 30 IPMBs, 25 noninvasive IPMCs, and 27 invasive IPMCs. The clinicopathologic features of the patients are summarized in Table 1. The neoplasms showed a tendency to arise in the pancreas head in elderly men. Larger cysts, mural nodules, and main duct type were significantly correlated with malignancy. These findings are consistent with previous reports (5, 18). This group can therefore be considered as an average population of IPMNs.

Chk2 phosphorylation in IPMNs. All of the IPMAs showed nuclear staining for phospho-Chk2, whereas normal ductal epithelia in 31 of 119 (26%) cases were positive for phospho-Chk2, indicating that the DNA damage checkpoint was fully activated in adenoma. With progression of atypia, the rate of phospho-Chk2 staining decreased: 46 of 46 (100%) of IPMAs, 29 of 30 (96.7%) of IPMBs, 21 of 25 (84.0%) of noninvasive

Table 1. Clinicopathologic features

	IPMA (n = 46)	IPMB (n = 30)	IPMC		Total	P
			Noninvasive (n = 25)	Invasive (n = 27)		
Gender						
Male	28	19	14	18	79	
Female	18	11	11	9	49	0.8795
Age (y)						
Mean ± SD	64.3 ± 8.5	67.3 ± 7.4	68.3 ± 6.4	65.5 ± 9.1	66.0 ± 8.1	0.1689
Location						
Head	26	21	20	18	85	
Body or tail	20	9	4	8	41	
Whole pancreas	0	0	1	1	2	0.6780
Distribution						
Main duct type	8	7	9	10	34	
Branch type	36	21	16	11	84	
Combined type	2	2	0	6	10	0.0119*
Size (mm)						
Median (25%, 75%)	25.5 (15.0, 35.0)	26.5 (20.0, 40.0)	36.0 (30.0, 50.0)	33.5 (28.0, 47.0)	30.0 (20.0, 40.0)	0.0003*
Mural nodule						
Present	7	13	15	19	54	
Absent	39	17	10	8	74	<0.0001*

*Statistically significant.

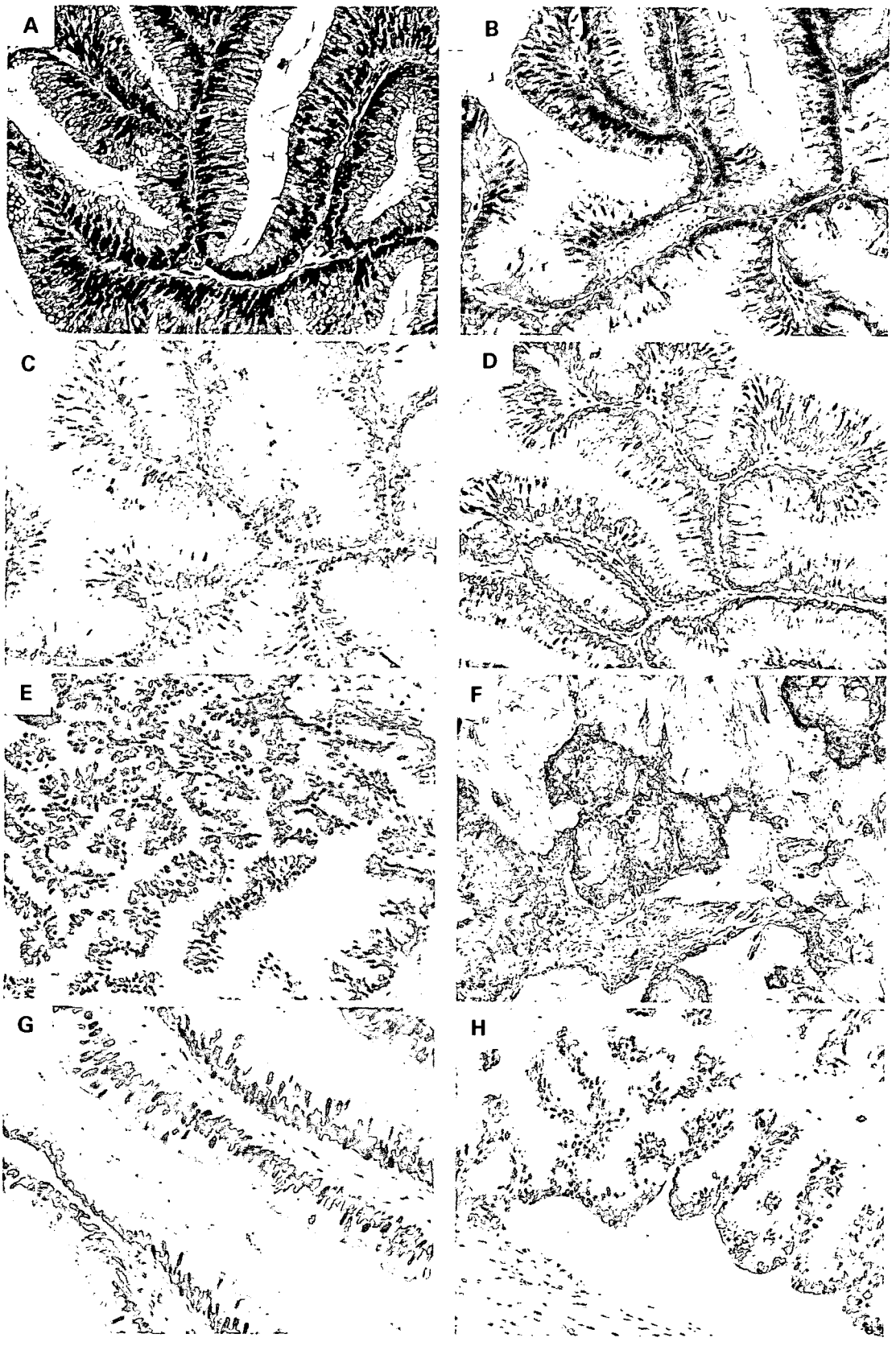

Fig. 3. *A* to *D*, IPMB. *A*, H&E stain. *B*, positive nuclear stain for phospho-Chk2. *C*, positive nuclear stain for Chk2. *D*, positive nuclear stain for ATM. *E*, noninvasive IPMC showing positive stain for phospho-Chk2. *F*, invasive IPMC showing negative stain for phospho-Chk2. *G*, IPMB showing positive nuclear stain for $p21^{WAF1}$. *H*, noninvasive IPMC showing positive nuclear stain for p53.

IPMCs, and 16 of 27 (59.9%) of invasive IPMCs (Figs. 3A, B, E, and F and 4A). The Cochran-Armitage test showed a significant decreasing trend between adenoma and invasive carcinoma ($P < 0.0001$). Less atypical lesions around phospho-Chk2–negative areas showed phospho-Chk2 staining. This suggests that activation of Chk2 is gradually disrupted in the transition to malignancy.

ATM and Chk2 protein expression. To investigate the cause of the loss of phospho-Chk2 staining, immunohistochemistry for Chk2 and ATM expression was done. Chk2 showed nuclear staining, whereas ATM showed nuclear and/or cytoplasmic staining. Chk2 expression was preserved in all tumors except one noninvasive IPMC (Figs. 3A and C and 4B), and ATM expression was preserved in all except one case of invasive IPMC (Figs. 3A and D and 4C). Both cases were negative for phospho-Chk2 staining and exhibited positive staining in surrounding less atypical lesions. Normal ductal epithelia in all cases were positive for both antibodies (Fig. 4B and C).

$p21^{WAF1}$ expression and p53 accumulation. To investigate downstream of Chk2, we studied $p21^{WAF1}$ expression and p53 accumulation. Normal epithelia in 7 of 119 (6%) cases were positive for $p21^{WAF1}$. Forty-one IPMAs (89%), 21 IPMBs (70%), 16 noninvasive IPMCs (64%), and 11 invasive IPMCs (41%) exhibited $p21^{WAF1}$ expression (Figs. 3G and 4D). $p21^{WAF1}$ expression showed a significant decreasing trend between adenoma and invasive carcinoma ($P < 0.0001$). Accumulation of p53 was seen in no normal epithelia (0%), one IPMA (2%), no IPMB (0%), five noninvasive IPMCs (20%), and eight invasive IPMCs (30%) and was shown to have an increasing tendency (Figs. 3H and 4E; $P < 0.0001$).

Discussion

In this study, we showed that Chk2 was phosphorylated in most of the IPMNs, including all cases of adenoma. Although Chk2 was originally reported to be phosphorylated in response to DNA double-strand breaks, recent studies have shown Chk2 phosphorylation in tumors of the lung, urinary bladder, colon, breast, and skin (10, 11, 15, 19). Chk2 phosphorylation has even been detected in preneoplastic lesions of the lung and skin (11). These findings suggest that the DNA damage checkpoint pathway is activated in the early stage of neoplasia, and our present data were consistent with this. However, the mechanism of Chk2 phosphorylation in neoplasms remains to be elucidated. Bartkova et al. (10) proposed that oncogene-induced DNA damage and telomere dysfunction activate the DNA damage pathway, and Gorgoulis et al. (11) mentioned that DNA replication stress due to aberrant stimulation of cell proliferation induces DNA damage. It has been reported that activation of oncogenes, such as *KRAS* mutation or c-erbB-2 overexpression, occurs in the early stage of IPMN (20–22). Recently, mutated *HRAS* was reported to activate the ATM-Chk2 pathway in both human fibroblast cultures and mouse keratinocyte tumor models (23, 24). Mutated *KRAS* might have similar effects on the DNA damage checkpoint activation in IPMNs because *KRAS* has a high degree of sequential analogy with *HRAS* and mutated forms of *HRAS* and *KRAS* have similar abilities to cause morphologic and growth transformation in cultured cells (25, 26). Unexpectedly, even normal ductal epithelia showed positive staining for phospho-Chk2 in some cases, but the proportion of these cases was much lower. It is

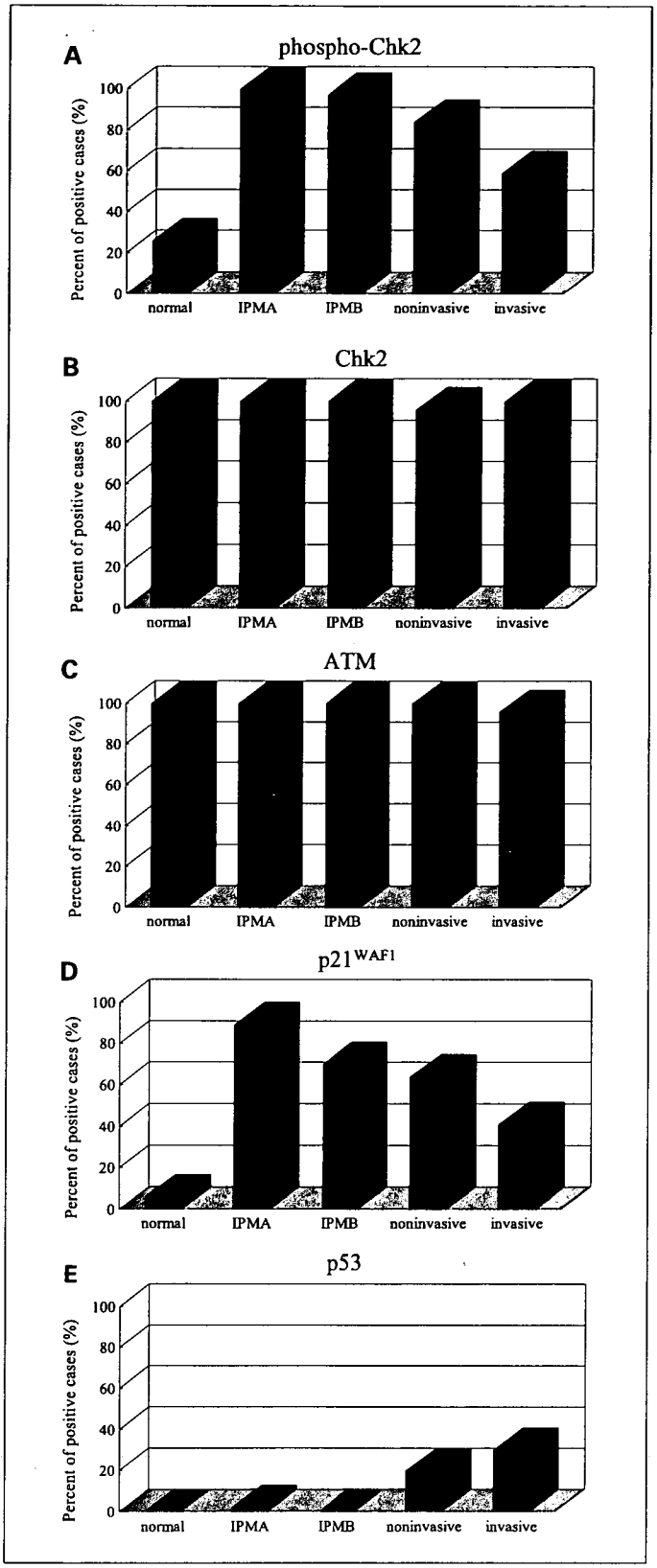

Fig. 4. Results of immunohistochemical analysis. *A*, phospho-Chk2 staining showed a significant decreasing trend ($P < 0.0001$, Cochran-Armitage test). *B*, one phospho-Chk2–negative noninvasive IPMC showed Chk2-negative staining. *C*, one phospho-Chk2–negative IPMC with invasion showed ATM-negative staining. *D*, p21 expression showed a significant decreasing trend ($P < 0.0001$, Cochran-Armitage test). *E*, p53 accumulation showed a significant increasing trend ($P < 0.0001$, Cochran-Armitage test).

therefore reasonable to conclude that the DNA damage checkpoint is activated in neoplasms. Although some reports have documented that Chk2 was not phosphorylated in normal tissue (e.g., lung, urinary bladder, and breast), others have documented that Chk2 was phosphorylated in normal bone marrow, testicular, and esophageal tissue (10, 11, 19, 27). Unlike lymphocytes in bone marrow and stem cells in testes, which undergo physiologic DNA double-strand breaks, the process of Chk2 activation in the normal esophageal epithelium remains unclear. There is also no evidence supporting physiologic DNA damage in pancreatic ductal epithelium. Considering the multifocal lesions and the frequent recurrence after margin negative resection of IPMNs, some of the morphologically normal ductal epithelium in the vicinity of the IPMN may already have activated oncogenes and hence show activation of the DNA damage response (5, 28).

In our study, Chk2 showed a decreasing trend of phosphorylation with the progression of IPMNs. In addition, $p21^{WAF1}$ expression decreased and p53 accumulation increased in the transition of IPMN from benign tumor to malignancy. Aberrations of the DNA damage checkpoint pathway are frequently recognized in malignant IPMNs, suggesting that checkpoint pathway disruption contributes to the IPMN progression. Bartkova et al. (10) reported a decrease of Chk2 phosphorylation in advanced urinary bladder carcinoma. Gorgoulis et al. (11) found that some lung cancers and melanomas showed no phospho-Chk2 staining, whereas their precursor lesions did. Our data indicate that, in some cases, loss of phospho-Chk2 staining could be attributed to ATM or Chk2 protein depletion. However, the cause of Chk2 inactivation in the other cases is uncertain. Loss of p53-binding protein 1 expression might prevent Chk2 phosphorylation, as concomitant defects of p53-binding protein 1 expression and Chk2 phosphorylation have been reported in lung cancer and melanoma (11, 19). Alternatively, it is possible that phosphatases, such as Wip1, are involved in Chk2 dephosphorylation (29).

In the present study, expression of the cyclin-dependent kinase inhibitor $p21^{WAF1}$ exhibited a gradual decline parallel to phospho-Chk2 staining. Down-regulation of $p21^{WAF1}$ according to tumor progression has been reported in gastric and colonic neoplasms, and expression of $p21^{WAF1}$ is regulated by Chk2 via both p53-dependent and p53-independent pathways (30–33). The reduction of $p21^{WAF1}$ expression observed in this study is thought to reflect inactivation of the DNA damage checkpoint pathway in IPMNs. Biankin et al. (34) reported an increasing trend of $p21^{WAF1}$ in intraepithelial neoplasia associated with invasive ductal carcinoma of the pancreas, but the genetic differences between invasive ductal carcinoma and IPMNs might account for this discordance.

p53 abnormalities in IPMNs are documented in the literature (6, 20, 35). Although p53 accumulation is less common in IPMNs than in pancreatic invasive ductal carcinoma, some IPMNs show it (36). Similar to our data, the frequency of p53 accumulation increased in malignant IPMNs. Halazonetis (12) proposed that frequent p53 inactivation in human cancer cells is due to DNA damage checkpoint activation. Without DNA damage checkpoint pathway activation, there would be no selective pressure for p53 dysfunction. In other words, *p53* mutation in malignant IPMNs supports activation of the DNA damage checkpoint in IPMNs.

It has been shown that Chk2 activation leads to cellular senescence (32, 33, 37). Senescence is a state of permanent cell cycle arrest accompanied by specific morphologic alterations and has been reported to be induced by certain oncogenes, such as *Ras* (38, 39). Recently, several authors have shown that senescence occurs in premalignant tumor cells and plays a role in limiting carcinogenesis, and they have suggested that attenuation of senescence due to deficiency of its effectors

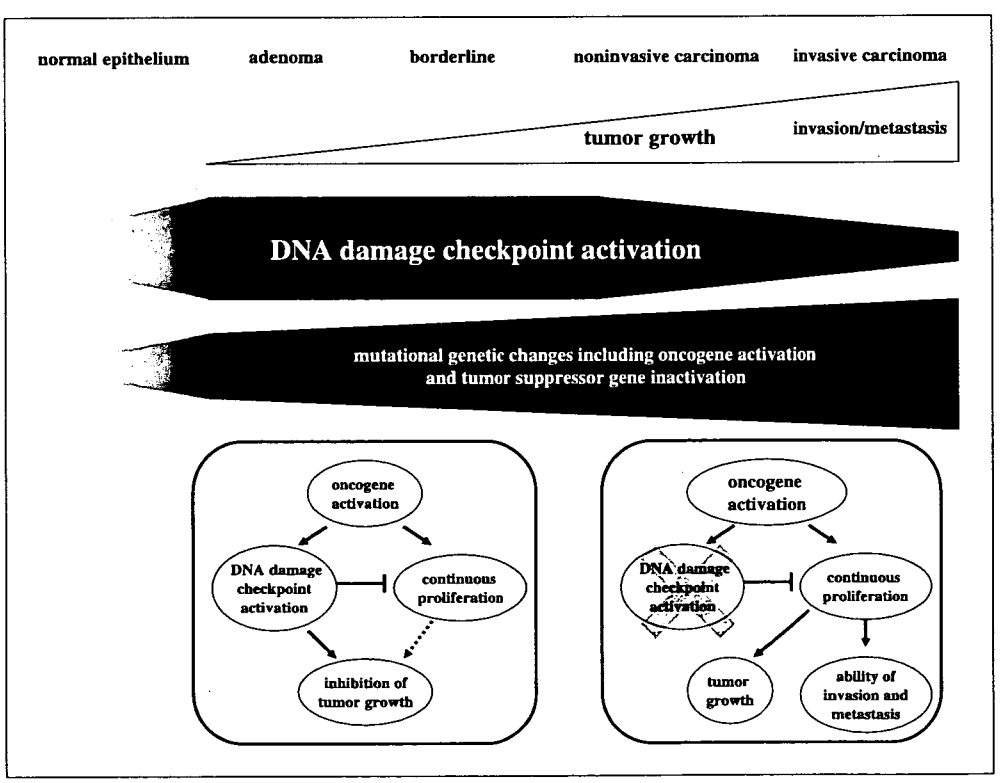

Fig. 5. Schema of hypothesis for the progression of IPMNs. In premalignant IPMNs, DNA damage checkpoint activation inhibits oncogene-induced cell proliferation and tumor growth. Activated oncogenes and disruption of the checkpoint pathway due to dysfunction of checkpoint-related molecules or phosphatase overexpression result in continuous cell proliferation, which leads to explosive tumor growth and acquisition of invasiveness and metastatic abilities.

results in progression to malignancy (40–42). It has been reported that the DNA damage checkpoint pathway is involved in the induction of oncogene-induced senescence and that inactivation of the DNA damage checkpoint due to suppression of mediator proteins, such as ATM, terminates senescence (23, 24). Our data showed that both Chk2 activation and expression of $p21^{WAF1}$, which is reported to be a senescence effector protein, reached a peak in adenoma lesions and they decreased gradually in the progression to invasive malignancy (33). It is therefore suggested that premalignant IPMNs may undergo senescence and that disruption of senescence might lead to malignancy.

We hypothesize a model for the progression of IPMNs as shown in Fig. 5. In premalignant IPMN, the activated DNA damage checkpoint inhibits oncogene-induced cell proliferation. Inactivation of the DNA damage checkpoint leads to continuous proliferation of tumor cells. Sustained replication increases the occurrence of molecular abnormalities, and shortage of nutrients due to the increased cell population might provide selective pressure for molecular abnormalities that enable cells to invade or metastasize (43). In other words, disruption of the DNA damage checkpoint results in acquisition of the characteristics of malignancy. Considering the good prognosis of benign and borderline lesions, development of methods to maintain the DNA damage checkpoint would enable us to avoid the use of invasive treatment. Detailed exploration of the molecular abnormalities leading to DNA damage checkpoint inactivation, such as dysfunction of p53-binding protein 1 and overexpression of Wip1, will contribute to progress in the treatment of IPMNs.

References

1. Longnecker DS, Adler G, Hruban RH, Kloeppel G. Intraductal papillary-mucinous neoplasms of the pancreas. In: Hamilton SR, Aaltonen LA, editors. Pathology and genetics of tumors of the digestive system. Lyon: IARC Press; 2000. p. 237–40.
2. Hruban RH, Takaori K, Klimstra DS, et al. An illustrated consensus on the classification of pancreatic intraepithelial neoplasia and intraductal papillary mucinous neoplasms. Am J Surg Pathol 2004;28:977–87.
3. Nagai E, Ueki T, Chijiiwa K, Tanaka M, Tsuneyoshi M. Intraductal papillary mucinous neoplasms of the pancreas associated with so-called "mucinous ductal ectasia." Histochemical and immunohistochemical analysis of 29 cases. Am J Surg Pathol 1995;19:576–89.
4. Niijima M, Yamaguchi T, Ishihara T, et al. Immunohistochemical analysis and *in situ* hybridization of cyclooxygenase-2 expression in intraductal papillary-mucinous tumors of the pancreas. Cancer 2002;94:1565–73.
5. Sohn TA, Yeo CJ, Cameron JL, et al. Intraductal papillary mucinous neoplasms of the pancreas: an updated experience. Ann Surg 2004;239:788–97; discussion 97–9.
6. Biankin AV, Biankin SA, Kench JG, et al. Aberrant p16(INK4A) and DPC4/Smad4 expression in intraductal papillary mucinous tumours of the pancreas is associated with invasive ductal adenocarcinoma. Gut 2002;50:861–8.
7. House MG, Guo M, Iacobuzio-Donahue C, Herman JG. Molecular progression of promoter methylation in intraductal papillary mucinous neoplasms (IPMN) of the pancreas. Carcinogenesis 2003;24:193–8.
8. Matsuoka S, Huang M, Elledge SJ. Linkage of ATM to cell cycle regulation by the Chk2 protein kinase. Science 1998;282:1893–7.
9. Ahn JY, Schwarz JK, Piwnica-Worms H, Canman CE. Threonine 68 phosphorylation by ataxia telangiectasia mutated is required for efficient activation of Chk2 in response to ionizing radiation. Cancer Res 2000;60:5934–6.
10. Bartkova J, Horejsi Z, Koed K, et al. DNA damage response as a candidate anti-cancer barrier in early human tumorigenesis. Nature 2005;434:864–70.
11. Gorgoulis VG, Vassiliou LV, Karakaidos P, et al. Activation of the DNA damage checkpoint and genomic instability in human precancerous lesions. Nature 2005;434:907–13.
12. Halazonetis TD. Constitutively active DNA damage checkpoint pathways as the driving force for the high frequency of p53 mutations in human cancer. DNA Repair (Amst) 2004;3:1057–62.
13. Kastan MB, Bartek J. Cell-cycle checkpoints and cancer. Nature 2004;432:316–23.
14. Vogelstein B, Lane D, Levine AJ. Surfing the p53 network. Nature 2000;408:307–10.
15. Eymin B, Claverie P, Salon C, et al. p14ARF activates a Tip60-dependent and p53-independent ATM/ATR/CHK pathway in response to genotoxic stress. Mol Cell Biol 2006;26:4339–50.
16. Arlehag L, Adell G, Knutsen A, Thorstenson S, Sun XF. ATM expression in rectal cancers with or without preoperative radiotherapy. Oncol Rep 2005;14:313–7.
17. Biankin AV, Kench JG, Biankin SA, et al. Pancreatic intraepithelial neoplasia in association with intraductal papillary mucinous neoplasms of the pancreas: implications for disease progression and recurrence. Am J Surg Pathol 2004;28:1184–92.
18. Tanaka M, Kobayashi K, Mizumoto K, Yamaguchi K. Clinical aspects of intraductal papillary mucinous neoplasm of the pancreas. J Gastroenterol 2005;40:669–75.
19. DiTullio RA, Jr., Mochan TA, Venere M, et al. 53BP1 functions in an ATM-dependent checkpoint pathway that is constitutively activated in human cancer. Nat Cell Biol 2002;4:998–1002.
20. Sessa F, Solcia E, Capella C, et al. Intraductal papillary-mucinous tumours represent a distinct group of pancreatic neoplasms: an investigation of tumour cell differentiation and K-ras, p53 and c-erbB-2 abnormalities in 26 patients. Virchows Arch 1994;425:357–67.
21. Hoshi T, Imai M, Ogawa K. Frequent K-ras mutations and absence of p53 mutations in mucin-producing tumors of the pancreas. J Surg Oncol 1994;55:84–91.
22. Sakai Y, Yanagisawa A, Shimada M, et al. K-ras gene mutations and loss of heterozygosity at the p53 gene locus relative to histological characteristics of mucin-producing tumors of the pancreas. Hum Pathol 2000;31:795–803.
23. Bartkova J, Rezaei N, Liontos M, et al. Oncogene-induced senescence is part of the tumorigenesis barrier imposed by DNA damage checkpoints. Nature 2006;444:633–7.
24. Di Micco R, Fumagalli M, Cicalese A, et al. Oncogene-induced senescence is a DNA damage response triggered by DNA hyper-replication. Nature 2006;444:638–42.
25. Kaplan JB. Biological activity of human N-ras and K-ras genes containing the Asn^{17} dominant negative mutation. Oncol Res 1994;6:611–5.
26. Oldham SM, Clark GJ, Gangarosa LM, Coffey RJ, Jr., Der CJ. Activation of the Raf-1/MAP kinase cascade is not sufficient for Ras transformation of RIE-1 epithelial cells. Proc Natl Acad Sci U S A 1996;93:6924–8.
27. Bartkova J, Bakkenist CJ, Rajpert-De Meyts E, et al. ATM activation in normal human tissues and testicular cancer. Cell Cycle 2005;4:838–45.
28. Salvia R, Crippa S, Falconi M, et al. Branch-duct intraductal papillary mucinous neoplasms of the pancreas: to operate or not to operate? Results of a prospective protocol on the management of 109 consecutive patients. Gut. In press 2006.
29. Oliva-Trastoy M, Berthonaud V, Chevalier A, et al. The Wip1 phosphatase (PPM1D) antagonizes activation of the Chk2 tumour suppressor kinase. Oncogene 2007;26:1449–58.
30. Oya M, Yao T, Tsuneyoshi M. Expressions of cell-cycle regulatory gene products in conventional gastric adenomas: possible immunohistochemical markers of malignant transformation. Hum Pathol 2000;31:279–87.
31. Doglioni C, Pelosio P, Laurino L, et al. p21/WAF1/CIP1 expression in normal mucosa and in adenomas and adenocarcinomas of the colon: its relationship with differentiation. J Pathol 1996;179:248–53.
32. Gire V, Roux P, Wynford-Thomas D, Brondello JM, Dulic V. DNA damage checkpoint kinase Chk2 triggers replicative senescence. EMBO J 2004;23:2554–63.
33. Aliouat-Denis CM, Dendouga N, Van den Wyngaert I, et al. p53-independent regulation of p21Waf1/Cip1 expression and senescence by Chk2. Mol Cancer Res 2005;3:627–34.
34. Biankin AV, Kench JG, Morey AL, et al. Overexpression of p21 (WAF1/CIP1) is an early event in the development of pancreatic intraepithelial neoplasia. Cancer Res 2001;61:8830–7.
35. Fujii H, Inagaki M, Kasai S, et al. Genetic progression and heterogeneity in intraductal papillary-mucinous neoplasms of the pancreas. Am J Pathol 1997;151:1447–54.
36. Fukushima N, Mukai K, Sakamoto M, et al. Invasive carcinoma derived from intraductal papillary-mucinous carcinoma of the pancreas: clinicopathologic and immunohistochemical study of eight cases. Virchows Arch 2001;439:6–13.
37. d'Adda di Fagagna F, Reaper PM, Clay-Farrace L, et al. A DNA damage checkpoint response in telomere-initiated senescence. Nature 2003;426:194–8.
38. Lowe SW, Cepero E, Evan G. Intrinsic tumour suppression. Nature 2004;432:307–15.
39. Serrano M, Lin AW, McCurrach ME, Beach D, Lowe SW. Oncogenic ras provokes premature cell senescence associated with accumulation of p53 and p16INK4a. Cell 1997;88:593–602.
40. Collado M, Gil J, Efeyan A, et al. Tumour biology: senescence in premalignant tumours. Nature 2005;436:642.
41. Michaloglou C, Vredeveld LC, Soengas MS, et al. BRAFE600-associated senescence-like cell cycle arrest of human naevi. Nature 2005;436:720–4.
42. Chen Z, Trotman LC, Shaffer D, et al. Crucial role of p53-dependent cellular senescence in suppression of Pten-deficient tumorigenesis. Nature 2005;436:725–30.
43. Karpinets TV, Foy BD. Tumorigenesis: the adaptation of mammalian cells to sustained stress environment by epigenetic alterations and succeeding matched mutations. Carcinogenesis 2005;26:1323–34.

Anti-patched-1 Antibodies Suppress Hedgehog Signaling Pathway and Pancreatic Cancer Proliferation

MASAFUMI NAKAMURA[1], MAKOTO KUBO[1], KOSUKE YANAI[1], YOSHIKO MIKAMI[1], MIO IKEBE[1], SHUNTARO NAGAI[1], KOJI YAMAGUCHI[2], MASAO TANAKA[2] and MITSUO KATANO[1]

Departments of [1]Cancer Therapy and Research, and [2]Surgery and Oncology, Graduate School of Medical Sciences, Kyushu University, Fukuoka, Japan

Abstract. *Background: The hedgehog (Hh) signaling pathway is aberrantly activated in many human carcinomas including pancreatic cancer and regulates tumor cell growth. Over-production of sonic hedgehog (Shh), a ligand of the Hh signaling pathway, increases the Hh signaling activity through transmitting the signal to patched-1 (Ptch1), the receptor of the Hh signaling pathway. Materials and Methods: α-Ptch1 antibodies were raised against an oligo-peptide, designed according to the Ptch1 amino-acid sequence. The specificity of α-Ptch1 was examined by immunoblotting and immuno-fluorescence, and biological effects were detected by RT-PCR and cell proliferation assay using two pancreatic cancer cell lines, Panc1 and SUIT-2. Results: α-Ptch1 recognized a 160 kDa protein as shown by immunoblotting and cell surface staining of pancreatic cancer cells. Incubation with α-Ptch1 suppressed Hh signaling activity and proliferation of pancreatic cancer cells. Conclusion: These results provide a new strategy for controling Hh dependent development of pancreatic cancer and other Hh related carcinomas.*

Pancreatic cancer is one of the most lethal human carcinomas with overall 5-year survival rate of <5%, partially because of the difficulty of diagnosis at an early stage (1). Despite the complete surgical removal of the tumor, most patients develop the disease again as metastases or local recurrence (2). Thus, it is a task of great urgency to establish a new medical strategy for the treatment of pancreatic cancer.

Abbreviations: Hh, hedgehog; Shh, sonic hedgehog; Ptch1, patched-1; Smo, smoothened; α-Ptch1, antibodies against patched1.

Correspondence to: Masafumi Nakamura, Department of Cancer Therapy and Research, Graduate School of Medical Sciences, Kyushu University, 3-1-1 Maidashi, Higashi-Ku, Fukuoka 812-8582, Japan. Tel: +81 92 642 6941, Fax: +81 92 642 6221, e-mail: mnaka@surg1.med.kyushu-u.ac.jp

Key Words: Pancreatic cancer, hedgehog signaling pathway, patched-1, sonic hedgehog, antibodies.

Recently, the hedgehog (Hh) signaling pathway has been reported to be aberrantly activated in pancreatic cancer in a ligand dependent manner (3-9). Without ligand stimuli, transmembrane protein patched-1 (Ptch1) suppresses another transmembrane protein smoothened (Smo), resulting in the silencing of the signal. In pancreatic cancer cells, aberrantly over produced sonic hedgehog (Shh), one of three Hh ligands, binds Ptch1 and inhibits the suppressive effect of Ptch1 on Smo, which activates Gli (glioma-associated oncogene) to transcript Hh target genes (6). The activated Hh signaling pathway promotes tumor cell growth, metastases and invasion. The Smo antagonist cyclopamine has been shown to inhibit the Hh signaling pathway, and suppress tumor cell growth *in vitro* (6) and in xenografts (4). Cyclopamine also increased the E-cadherin level and reduced the invasive ability of pancreatic cancer cells *in vitro*, and inhibited the metastatic spread of immortal pancreatic cells stably over-expressing Gli1 in a xenograft model (2). These findings indicate that the Hh signaling pathway is a useful theraputic target in human pancreatic cancer. However cyclopamine is an alkaloid and not precisely targeting the hedgehog pathway.

Antibodies which recognize an oligopeptide of Ptch1 on the cancer cell surface and have the ability to silence Shh stimuli to Ptch1 were raised in the present study. The aim was to find a new strategy for controling pancreatic cancer and other Hh dependent carcinomas by precisely controling the Hh activity to avoid the side effects. The antibodies might be also useful as a tool of marking and targeting cancer-cell surface *in vivo* for the diagnosis and the drug-delivery system of anti-cancer drugs.

Materials and Methods

Cell culture, reagents and antibodies. Human pancreatic cancer cell lines (Panc1 and SUIT-2), and human breast carcinoma cell lines (SK-BR-3, BT-474, MCF-7 and MDA-MB-231) were maintained at 37°C under a humidified atmosphere of 5% CO_2 and 95% air in RPMI 1640 medium (Life Technologies, Grand Island, NY, USA) supplemented with 10% fetal bovine serum (FBS, Life Technologies)

and antibiotics (100 units/mL penicillin, and 100 μg/mL streptomycin Meijiseika, Tokyo, Japan). Anti-Ptch1 anti-serum (α-Ptch1) was prepared by Sigma (Deisenhofen, Germany) by the KLH (keyhole limpet hemacyamin)-MBS method (10), briefly, an oligo-peptide customized according to the amino-acid sequence of Ptch1 (KADYPNIQH) as an antigen was conjugated to the KLH by cystein and injected to rabbits. Rabbit serum was collected before (pre-serum) and after (α-Ptch1) immunization. Another anti-Ptch1 serum (G-19) was purchased from Santa Cruz Biotechnology (Santa Cruz, CA, USA).

Immunoblotting. Whole-cell extraction was performed with M-PER® Reagents (Pierce Biotechnology, Rockford, IL, USA) according to the manufacturer's instructions. Protein concentration was determined with a Bio-Rad Protein Assay (Bio-Rad Laboratories, Hercules, CA, USA) and the whole-cell extract (100 μg) was separated by electrophoresis on SDS-polyacrylamide gel and transferred to Protran nitrocellulose membranes (Schleicher & Schnell BioScience, Dassel, Germany). Blots were then incubated with pre-serum (1:500), α-Ptch1 (1:500) or G-19 (1:500) as primary antibodies overnight at 4°C. Then the blots were incubated with horseradish peroxidase-linked secondary antibodies (Amersham Biosciences, Piscataway, NJ, USA) at room temperature for 1 h. Immunocomplexes were detected with an ECL® plus Western Blotting Detection System (Amersham Biosciences) and visualized with a Molecular Imager FX (Bio-Rad).

Immunostaining of cell line. Panc1 cells ($2x10^4$/well) were seeded onto pre-underlaid Poly-L-lysine coated cover glass (Asahi Techno Glass Corporation, Chiba, Japan) in 24-well plates and were incubated overnight in 10% FBS-RPMI. Immunostaining was performed as previously described with some modification (11). In brief, cells were fixed in 4% paraformaldehyde followed by permeabilization with 0.2% Triton X-100 and incubated with primary antibodies (α-Ptch1 or pre-serum) followed by secondary antibodies. After mounting in Vectorshield Mounting Medium (Vector Laboratories, Burlingame, CA, USA), samples were examined by Laser confocal microscopy (Nikon ECLIPS E600, Tokyo, Japan). Exposure time for recording was manually fixed to be the same for pre-serum and α-Ptch1. The antibodies and dilutions used were as follows: pre-serum (1/200) or α-Ptch1 (1/200) and AlexaFluor 488 goat anti-rabbit IgG (1:400; Molecular Probes, Eugene, OR, USA).

Reverse transcription-polymerase chain reaction (RT-PCR). RT-PCR was performed according to a method described previously (9). Briefly, total RNA was extracted from each cell line with the guanidinium thiocyanate-phenol-chloroform single-step method. For the reverse transcription reaction, pd(N)6 Random Hexamer (GE Healthcare UK Ltd, Buckinghamshire, England) were used for priming. *Gli1* sense (5'-TCT GCC CCC ATT GCC CAC TTG -3') and antisense (5'-TAC ATA GCC CCC AGC CCA CTT G-3') primers yielded a 480-bp product. *Ptch1* sense (5'-CGG CGT TCT CAA TGG GCT GGT TTT-3') and antisense (5'-GTG GGG CTG CTG TCT CGG GTT CG-3') primers yielded a 376-bp product. *β-Actin* sense (5'-CCA GGC ACC AGG GCG TGA TG-3') and antisense (5'-CGG CCA GCC AGG TCC AGA CG-3') primers gave rise to a 436-bp product. Amplification conditions comprised an initial denaturation for 2 min at 94°C followed by 30 cycles of 94°C for 30 sec, 58°C for 30 sec, and 72°C for 1 min. Amplification of each gene was in the linear range. The RT-PCR products were separated on ethidium bromide-stained 2% agarose gels. Semi-quantitative analysis was done with Molecular Imager FX Pro (Bio-Rad).

Proliferation assay. Cells ($2x10^4$/well) seeded in 48-well plates in complete culture medium were incubated overnight. After a few brief washes with RPMI, the medium was changed to 2% FBS-RPMI containing α-Ptch1 or pre-serum. After incubation for 4 days, cells were harvested by trypsinization and viable cells were counted by flow cytometry [Coulter Counter (Beckman Coulter, Fullerton, CA, USA)].

Results

Immunoblotting analysis of α-Ptch1. An extract of Panc1, a pancreatic cancer cell line, was prepared as a source of Ptch1 protein, and subjected to immunoblotting. α-Ptch1 recognized a 160 kDa band of the Panc1 extract (Figure 1A) in contrast to the pre-serum control. Extracts of 4 breast cancer cell lines, SK-BR-3, BT-474, MCF-7 and MDA-MB-231, and Panc1, were subjected to immunoblotting with α-Ptch1 or G-19. α-Ptch1 visualized the same 160 kDa bands in all 5 extracts of the cancer cell lines, consistent with the band recognized by G-19 (Figure 1B). These results indicated that α-Ptch1 antibodies have affinity with Ptch1.

Cell surface protein recognition. The localization of the target protein recognized by α-Ptch1 was checked by immunofluorescence. α-Ptch1 exclusively stained the cell surfaces (Figure 2 middle) in the same pattern as phase contrast images (Figure 2 right). When the α-Ptch1 and phase contrast images were changed to green and red, respectively, overlying of both images showed a yellow color because of the colocalization of the two images (data not shown). In contrast pre-serum stained almost nothing (Figure 2 left). Since Ptch1 is located on the cell membrane, these images confirmed that α-Ptch1 specifically recognized Ptch1.

α-Ptch1 and activity of the Hh signal pathway in pancreatic cancer cells. The effect of α-Ptch1 on Hh signaling activity in pancreatic cancer cells was analyzed by RT-PCR. Because Gli1 and Ptch1 are not only the components of Hh signaling but also target genes of Gli1 trans-activation, the mRNA levels of Gli1 and Ptch1 as markers of the activity of Hh signaling pathway were examined. Panc1 cells were incubated with α-Ptch1, and subjected to RT-PCR. α-Ptch1 suppressed the expression levels of both Gli1 and Ptch1 in contrast to pre-serum, but did not suppress β-actin, an internal control (Figure 3).

Pancreatic cancer cell proliferation. Panc1 proliferation was suppressed by α-Ptch1 in comparison to pre-serum (Figure 4a). The suppressive effect of α-Ptch1 was further examined using a different pancreatic cancer cell line, SUIT-2. α-Ptch1 significantly suppressed proliferation of SUIT-2 in